Developmental Biology 441 (2018) 67–82

Contents lists available at ScienceDirect

Developmental Biology

journal homepage: www.elsevier.com/locate/developmentalbiology

Original research article

The transcription factor *Tfap2e*/AP-2ε plays a pivotal role in maintaining the identity of basal vomeronasal sensory neurons

Jennifer M. Lin, Ed Zandro M. Taroc, Jesus A. Frias, Aparna Prasad, Allison N. Catizone, Morgan A. Sammons, Paolo E. Forni*

Department of Biological Sciences, University at Albany, Albany, NY 12222, USA

A B S T R A C T

The identity of individual neuronal cell types is defined and maintained by the expression of specific combinations of transcriptional regulators that control cell type–specific genetic programs.

The epithelium of the vomeronasal organ of mice contains two major types of vomeronasal sensory neurons (VSNs): 1) the apical VSNs which express vomeronasal 1 receptors (V1r) and the G-protein subunit Gαi2 and; 2) the basal VSNs which express vomeronasal 2 receptors (V2r) and the G-protein subunit Gαo. Both cell types originate from a common pool of progenitors and eventually acquire apical or basal identity through largely unknown mechanisms.

The transcription factor AP-2ε, encoded by the *Tfap2e* gene, plays a role in controlling the development of GABAergic interneurons in the main and accessory olfactory bulb (AOB), moreover AP-2ε has been previously described to be expressed in the basal VSNs. Here we show that AP-2ε is expressed in post-mitotic VSNs after they commit to the basal differentiation program. Loss of AP-2ε function resulted in reduced number of basal VSNs and in an increased number of neurons expressing markers of the apical lineage. Our work suggests that AP-2ε, which is expressed in late phases of differentiation, is not needed to initiate the apical-basal differentiation dichotomy but for maintaining the basal VSNs' identity. In AP-2ε mutants we observed a large number of cells that entered the basal program can express apical genes, our data suggest that differentiated VSNs of mice retain a notable level of plasticity.

1. Introduction

The vomeronasal organ (VNO) is an olfactory sub-system of vertebrates specialized for the detection of pheromones. Each vomeronasal sensory neuron (VSN) selectively expresses only one or two vomeronasal receptors (VR) out of hundreds encoded by the V1r or V2r gene families (Silvotti et al., 2007), and are regenerated throughout life (Brann and Firestein, 2010; Giacobini et al., 2000; Oboti et al., 2015).

Neurons located within the apical region of the vomeronasal epithelium (Huilgol et al.) express V1rs (Dulac and Axel, 1995), the Gα-protein subunit Gαi2, the transcription factor (TF) Meis2 (Enomoto et al., 2011), and project to the anterior accessory olfactory bulb (AOB). VSNs distributed in the basal regions of the VNE, express V2Rs, Gαo, the TF AP-2ε (Enomoto et al., 2011), and project to the posterior AOB (Montani et al., 2013; Tirindelli and Ryba, 1996).

A common pool of Ascl-1+ neural progenitor cells (NPCs) resides at the lateral and basal margins of the VNE and generates neuronal precursors which differentiate into apical or basal VSNs (Cau et al., 1997; de la Rosa-Prieto et al., 2010; Martinez-Marcos et al., 2000; Murray et al., 2003). Although significant progress has been made in understanding the molecular basis of chemosensory detection, little information exists on how the terminal differentiation of apical and basal VSNs is established and cellular plasticity is restricted (Enomoto et al., 2011; Oboti et al., 2015).

The identity of specific neuronal cell types is defined and maintained by the sets of transcriptional regulators that control type–specific genetic programs (Hobert, 2016; Patel and Hobert, 2017). Bcl11b/Ctip2 is currently the only TF found to play a role in controlling VSN differentiation, as a permissive factor for the basal VSN program, as Bcl11b null mutants display a significant loss of immature basal neurons, increase of immature apical neurons, however an overall decrease in VSNs that reach maturity (Enomoto et al., 2011; Suarez, 2011). Moreover, Bcl11b nulls do not survive postnatally, limiting long-term analysis of defective differentiation on the VNE and AOB morphology and function. Microarray data from *Bcl11b* null mutants identified reduced expression of *Tfap2e* (AP-2ε), which has since been

* Corresponding author.
E-mail address: pforni@albany.edu (P.E. Forni).

https://doi.org/10.1016/j.ydbio.2018.06.007
Received 13 February 2018; Received in revised form 22 May 2018; Accepted 13 June 2018
Available online 19 June 2018
0012-1606/

proposed as a potential player in directing the apical-basal dichotomy in the VNO (Enomoto et al., 2011; Suarez, 2011), although never experimentally tested.

In this work, we exploited an AP-2ε null mouse line (Feng et al., 2009), where a Cre recombinase gene has been inserted into the endogenous AP-2ε genomic locus. Unlike Bcl11b null mice, AP-2ε nulls are viable with no gross structural abnormalities. We used this mouse line to determine the impact of AP-2ε loss-of-function on VSN terminal differentiation and circuit formation in the AOB at postnatal stages by following AP-2ε expression and genetic lineage.

We established that, in the accessory olfactory system, AP-2ε is expressed by post-mitotic neurons in the basal portion of the VNO and by the mitral cells of the anterior portion of the AOB. We demonstrated that AP-2ε plays a role in the maintenance of the identity and homeostasis of basal VSNs after differentiation, likely by repressing the apical genetic program.

2. Materials and methods

2.1. Animals

The AP-2εCre line (*Tfap2e*$^{tm1(cre)Will}$) were obtained from Dr. Trevor Williams, Department of Craniofacial Biology, University of Colorado, and characterized on a Black Swiss background (Feng et al., 2009). *(Rosa)26Sor*^{Tos} (B6.129×1-*Gt(ROSA)26Sor*$^{tm1(EYFP)Cos}$/J, JAX stock #00614; termed *R26*^{YFP}) reporter mice (Srinivas et al., 2001) and R26RtdTomato (B6.Cg-Gt(ROSA)26Sortm9$^{(CAG-tdTomato)Hze}$/J, JAX stock #007909) reporter mice (Madisen et al., 2010) were purchased from (Jackson Laboratories, Bar Harbor, ME). Lineage tracing experiments were done on littermate mice on Black Swiss/C57BL/6J mixed background. Mutant and wild-type mice of either sex were used. All mouse studies were approved by the University at Albany Institutional Animal Care and Use Committee (IACUC).

2.2. Tissue preparation

Tissue collected at ages ≥ P8 were perfused with PBS then 3.7% formaldehyde in PBS. Brain tissue was isolated at the time of perfusion and additionally immersion-fixed for 3–4 h at 4 °C. Noses were immersion fixed in 3.7% formaldehyde in PBS at 4 °C overnight then decalcified in 500 mM EDTA for 3–4 days. All samples were cryoprotected in 30% sucrose in PBS overnight at 4 °C then embedded in Tissue-Tek O.C.T. Compound (Sakura Finetek USA, Inc., Torrance CA) using dry ice, and stored at − 80 °C. Tissue was cryosectioned using a CM3050S Leica cryostat at 16 µm for VNOs and 20 µm for OBs and collected on VWR Superfrost Plus Micro Slides (Radnor, PA) for immunostaining and in situ hybridizations (ISH). All slides were stored at − 80 °C until ready for staining.

2.3. Immunohistochemistry

Citrate buffer (pH 6) microwave antigen retrieval (Forni et al., 2006) was performed, for all the antibodies indicated with asterisks (*). Primary antibodies and concentrations used in this study were, *Goat anti-AP-2ε (2 µg/mL, sc-131393 X, Santa Cruz, Dallas, TX) **Rat anti-BrdU (1:250, NB500-169, Novus Biologicals, Littleton, CO)* Rabbit anti-Cleaved Caspase-3 (1:1000, AB3623, Millipore, Darmstadt, Germany), *Mouse anti-Gαi2 (1:200, 05–1403, Millipore), Rabbit anti-Gαo (1:1000, 551, Millipore), Rabbit anti-GAP43 (1:500, 16053, Abcam, Cambridge, MA), Chicken anti-GFP (1:1000, ab13970, Abcam), Rabbit anti-GFP (1:2000, A-6455, Molecular Probes, Eugene, OR) *Rabbit anti-Ki67 (1:1000, AB9260, Millipore), *Mouse anti-Meis2 (1:500, sc-515470, Santa Cruz), *Mouse anti-NeuroD1 (1:100, sc-46684, Santa Cruz), Goat anti-Nrp2 (1:4000, AF567, R & D Systems, Minneapolis, MN), Goat anti-OMP (1:4000, 5441001, WAKO, Osaka, Japan), *Mouse anti-Tbx21 (1:400, sc-21749, Santa Cruz) Rabbit anti-V2R2 (1:4000, Gift from Dr. Roberto Tirindelli, Univ. degli Studi di Parma, Italy). Sections were pre-incubated 1.0 M HCl at 37° for 30 min prior to anti-BrdU immunostaining (Forni et al., 2011).

For chromogen-based reactions, tissue was stained as previously described (Forni et al., 2011.). Staining was visualized with the Vectastain ABC Kit (Vector, Burlingame, CA) using diaminobenzidine (DAB) (Forni et al., 2011); sections were counterstained with methyl green.

Species-appropriate secondary antibodies conjugated with either Alexa Fluor 488, Alexa Fluor 594, Alexa Fluor 568, Alexa Fluor 680 were used for immunofluorescence detection (Molecular Probes and Jackson ImmunoResearch Laboratories, Inc., Westgrove, PA). Sections were counterstained with 4′,6′-diamidino-2-phenylindole (DAPI) (1:3000; Sigma-Aldrich) and coverslips were mounted with FluoroGel (Electron Microscopy Services, Hatfield, PA). Confocal microscopy pictures were taken on a Zeiss LSM 710 microscope. Epifluorescence pictures were taken on a Leica DM4000 B LED fluorescence microscope equipped with a Leica DFC310 FX camera. Images were further analyzed using FIJI/ImageJ software.

2.4. In situ probes

Probes against transcripts derived from *Big2* and *Meis2* were donated to us by Dr. J Hirota, Tokyo Institute of Technology, Japan and prepared as previously described (Enomoto et al., 2011). Plasmids to generate probes specific for *Gao* and *Gαi2* were provided by J.F. Cloutier, McGill University, Montreal, Canada (Cloutier et al., 2004).

Sense and antisense probes against the full cDNA sequences of *Vmn1r73* (CCDS20800.1), *Vmn1r81* (CCDS20806.1), *Vmn1r82* (CCDS57493.1), and *Vmn1r84* (CCDS20808.1) were generated from double stranded DNA gene blocks containing the cDNA sequences of the genes of interest flanked by an upstream T7 (5′-TAATACGACTCACTATAGGG-3′) promoter and downstream SP6 (5′-TTCTATAGTGTCACCTAAAT-3′) promoter. These gene blocks were synthesized by Integrated DNA Technologies, Inc. (Coralville, Iowa).

2.5. PCR amplification of V1r in situ probe cassettes

10 ng of each synthesized cassette were amplified for 35 cycles using the NEB Q5 High-Fidelity 2X master mix (New England BioLabs, Ipswich, MA) according to manufacturer's specifications. Primers available in Supplementary Table S2. PCR products were size selected on a 1% agarose gel and purified (Zymo DNA Clean & Concentrator, Irvine, CA).

2.6. In situ hybridization

Digoxigenin-labeled RNA probes were prepared by *in vitro* transcription (DIG RNA labeling kit; Roche Diagnostics, Basel, Switzerland). In situ hybridizations were performed on 16 µm cryosections that were rehydrated in 1x PBS for 5 min, then fixed in 4% PFA in 0.1 M phosphate buffer for 20 min at 4 °C, treated with 10 µg/mL proteinase K (Roche) for 12 min at 37 °C, then refixed in 4% PFA at 4 °C for 20 min. To inactivate the internal alkaline phosphatase, the tissue was treated with 0.2 M HCl for 30 min. Nonspecific binding of the probe to slides was reduced by dipping slides in 0.1 M triethanolamine (pH 8.0)/0.25% acetic anhydride solution, then washed with 2x Saline-Sodium Citrate (SSC) buffer before incubating in hybridization solution for 2hrs at room temperature. Slides were then hybridized with 200 µl of probe in hybridization solution at 65 °C overnight in a moisture chamber. After hybridization, the slides were washed in 2x SSC, briefly, then in 1x SSC/50% formamide for 40 min at 65 °C. RNase A treatment (10 µg/mL) was carried out at 37 °C for 30 min. The slides were then washed with 2x SSC then 0.2x SSC for 15 min each at 65 °C. Hybridization was visualized by immunostaining with an alkaline

phosphatase conjugated anti-DIG (1:1000), and NBT/BCIP developer solution (Roche Diagnostics). After color reaction, the slides were put into 10 mM Tris-HCl pH 8.0/1 mM EDTA.

2.7. Microarray

The whole VNOs of P17 AP-2ε$^{-/-}$ nulls and wild-type controls (n ≥ 3 per genotype) were isolated, digested, and used to extract RNA using the PureLink™ RNA Mini Kit (Invitrogen by Life Technologies, Carlsbad, CA). RNA sample quality was tested using Agilent/2100 bioanalyzer. Whole transcriptome analysis was performed on Affymetrix Mouse Gene ST 2.0 at the Center of Functional Genomics, University at Albany, SUNY. Data analysis was performed using Transcriptome Analysis Console (TAC 4.0) Software, Applied Biosystems. Expression of selected genes of interest with significance p-value > 0.05 was further validated. Microarray data was deposited in GEO (GSE110083).

2.8. qRT-PCR

cDNA from Wildtype and AP-2ε null VNOs (n = 3 per genotype, P17) was generated from 1000 ng of RNA per biological replicate using the *Applied Biosystems* High Capacity cDNA kit (#4368814). Samples were amplified and measured using the *Bio-Rad iTaq Universal SYBR Green Supermix* and the *Applied Biosystems 7900HT* instrument. All samples were run with three technical replicates and a relative standard curve was generated by serially diluting the samples. All values are relative to the standard curve and normalized to *Gapdh*. Two-tailed, unpaired *t*-tests were performed between wildtype and knockout mouse data. qPCR primers for each of the genes analyzed are available in Table 1.

2.9. BrdU birthdating and cell fate tracking

Intraperitoneal (IP) BrdU injections (50 mg/kg) were performed on P7 control and null lineage traced mice on a mixed C57B/Black Swiss background. Samples were collected at P21 (post-injection day 14) as described in de la Rosa-Prieto et al. (2010). Immunostainings against BrdU, tdTomato, Gαo, and Gαi2 were performed and analyzed using FIJI software. Number of BrdU+ and BrdU+/tdTomato+ cells were quantified and averaged across three series per animal. Cell counts were performed as described in Section 2.10.

2.10. Quantification and statistical analyses of microscopy data

Measurements of VNE and cell counts were performed on confocal images or bright field images of coronal serial sections immunostained or underwent in situ hybridizations for the indicated targets. In animals ≥ P15, the most central 6–8 sections on the rostro-caudal axis of the VNO were quantified and averaged, and in animals ≥ P0, the most medial 4–6 sections were quantified and averaged. Measurements and cell counts were done using ImageJ.

Counts of Tbx21+ cells in the AOB and measurements of the glomerular layer areas were performed on parasagittal sections containing identifiable glomerular layers to distinguish between anterior and posterior MCL layers. Statistical differences between genotypes were quantified with two-tailed unpaired *t*-test using Prism 7.0b, (GraphPad Software, CA, USA).

Table 1
qRT-PCR Primer Sequences Sequences of primers used in qRT-PCR analysis (see Fig. 3C) for Gαo, Meis2, Vmn1r81, Vmn1r84, Vmn2r69, Vmn2r18, and Gapdh.

SEQUENCE (5′ → 3′)	Gene
CAGCCTGGATCGGATTGG	Guanine nucleotide binding protein, alpha O (Gαo) FWD
TGACTCTGGTTCGGAGGATGT	Guanine nucleotide binding protein, alpha O (Gαo) REV
TGAGCAAGGCGATGGGTTAG	Meis homeobox 2 FWD
TGTCTGGATCGTCGTCATCAC	Meis homeobox 2 REV
TGCCTACTGGGTTGTTTCCAA	Vomeronasal 1 receptor 81 FWD
TTGTGGCTCTGTGTTTAAGCATAAT	Vomeronasal 1 receptor 81 REV
CTCCTGGATGACCTCTTATGTAAACTT	Vomeronasal 1 receptor 84 FWD
GGTGCAGTGCAGGGAAATG	Vomeronasal 1 receptor 84 REV
GCACCATGATTCAGCTGATTCTC	Vomeronasal 2, receptor 69 FWD
TCACTGAACCTTTGTTGCAAACA	Vomeronasal 2, receptor 69 REV
ACTGGCACTAGGGAGCTTCACT	Vomeronasal 2, receptor 18 FWD
CTGCAGAACACCACCATACTGAAT	Vomeronasal 2, receptor 18 REV
AAGAAGGTGGTGAAGCAGGCATC	Gapdh FWD
CGAAGGTGGAAGAGTGGGAGTTG	Gapdh REV

2.11. Experimental design and statistical analysis

All data were collected from mice kept under similar housing conditions, in transparent cages on a normal 12 h. light/dark cycle. Tissue collected from either males or females were analyzed and no significant sex differences were observed, so the data from males and females in the same genotype/treatment group were combined; ages analyzed are indicated in text and figures. The data are presented as mean ± SEM. Prism 7.0b was used for statistical analyses, including calculation of mean values, and standard errors. Two-tailed, unpaired *t*-test were used for all statistical analyses, and calculated p-values < 0.05 were considered statistically significant. Sample sizes and p-values are indicated as single points in each graph and/or in figure legends.

3. Results

3.1. AP-2ε is expressed in basal VSNs

Immunohistochemistry on P8 mice revealed AP-2ε protein expression in the cells located in the most basal territories of the VNO (Fig. 1A). Stronger AP-2ε immunoreactivity was observed in the marginal neurogenic regions of the VNO where newly formed VSNs localize proximal to the proliferating precursor cells (Fig. 1A,B, Use Fig. 1K,L as reference). AP-2ε expression was also retained in mature neurons distal from the marginal zones, though at lower levels (Fig. 1A,B).

The G-protein subunit Gαo is selectively expressed in differentiated basal VSNs (Herrada and Dulac, 1997; Matsunami and Buck, 1997). Double immunohistochemistry against Gαo and AP-2ε showed selective and sustained AP-2ε expression in the basal VSNs (Fig. 1C). By using an AP-2ε$^{-/-}$ (AP-2ε–null/KO) mouse line, where the Cre recombinase transgene has been knocked into the AP-2ε coding sequence (Feng et al., 2009), we could follow the expression of non-functional AP-2ε using Cre as a proxy for AP-2ε expression. In AP-2ε$^{-/-}$ mice Cre immunoreactivity was found to be strongly expressed, as for AP-2ε in controls, in the marginal zones (Fig. 1D,E). However, in the AP-2ε$^{-/-}$ the distribution of the cells expressing Cre was not obviously segregated to the basal territories as Cre immunoreactivity was found in cells in both basal and apical regions, see immunoreactivity between dotted lines in Fig. 1D compare to Fig. 1A. Moreover, Cre immunoreactivity was nearly undetectable distal from the marginal zones, (Fig. 1A,D see zone 4/5 in controls and AP-2ε mutants, quantifications in Fig. 1 B-E).

Although Cre expression was found to overlap with AP-2ε in AP-2ε$^{+/-}$ (Fig. 2A-C), no AP-2ε immunoreactivity was found in the KOs (Fig. 1F).

The stronger immunoreactivity in the marginal zones suggested potential roles for AP-2ε in differentiation or in controlling maturation steps of basal VSNs. To further investigate at what stages of VSN development AP-2ε is expressed (Fig. 1K-L as a reference) we performed immunolabeling against AP-2ε and the proliferative cell marker, Ki67, the neuronal precursor marker, NeuroD1, and Gap43, which labels immature neurons forming neurites (Cau et al., 2002, 1997; Enomoto et al., 2011; Murray et al., 2003). We found AP-2ε

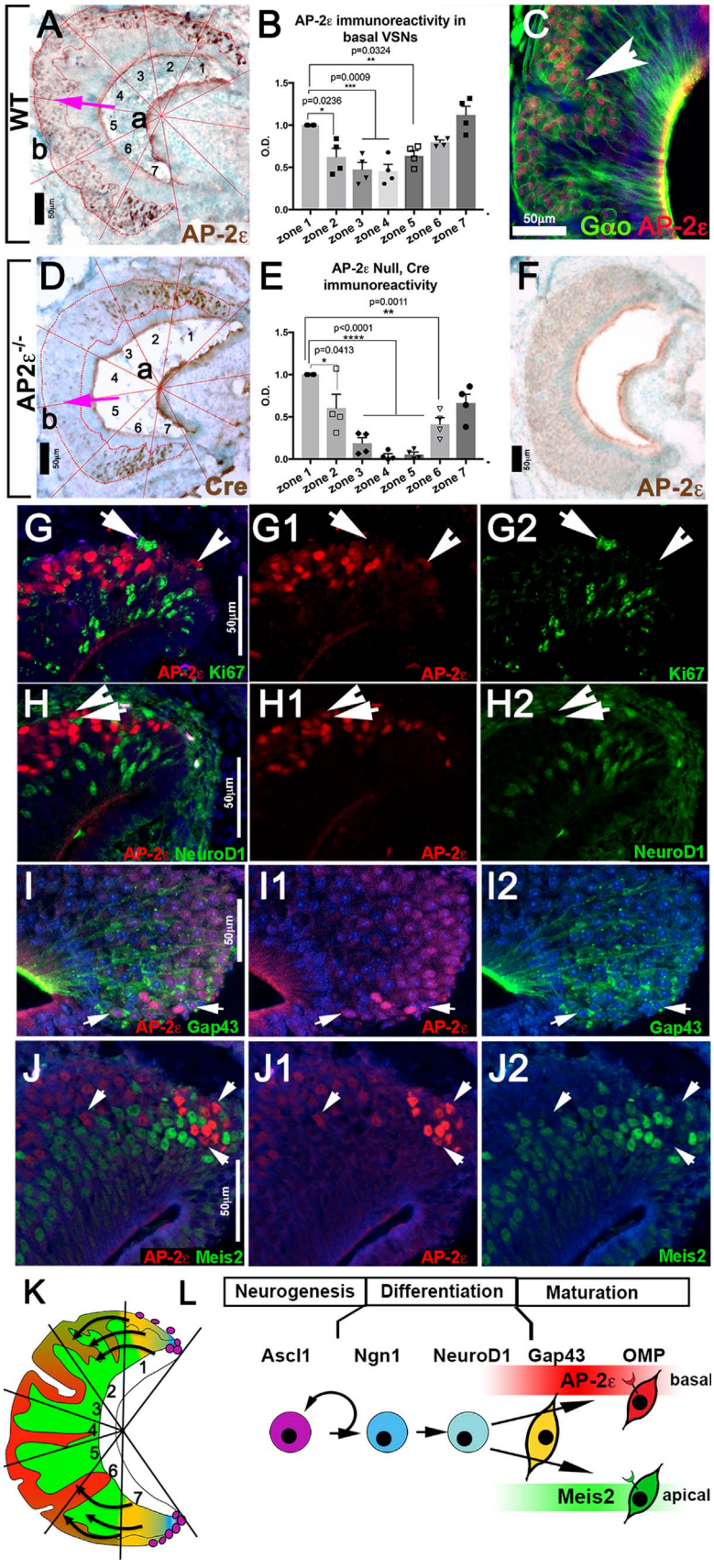
A
WT
a
b
1
2
3
4
5
6
7
50μm
AP-2ε
B
AP-2ε immunoreactivity in basal VSNs
p=0.0324
**
p=0.0009
***
p=0.0236
*
O.D.
1.5
1.0
0.5
0.0
zone 1
zone 2
zone 3
zone 4
zone 5
zone 6
zone 7
C
50μm
Gαo AP-2ε
D
AP2ε-/-
a
b
Cre
E
AP-2ε Null, Cre immunoreactivity
p=0.0011
**
p<0.0001
****
p=0.0413
*
F
AP-2ε
G
AP-2ε Ki67
G1
AP-2ε
G2
Ki67
H
AP-2ε NeuroD1
H1
AP-2ε
H2
NeuroD1
I
AP-2ε Gap43
I1
AP-2ε
I2
Gap43
J
AP-2ε Meis2
J1
AP-2ε
J2
Meis2
K
L
Neurogenesis
Differentiation
Maturation
Ascl1
Ngn1
NeuroD1
Gap43
OMP
AP-2ε
basal
Meis2
apical

Fig. 1. AP-2ε is expressed in differentiating basal vomeronasal sensory neurons (VSNs). Immunohistochemistry against AP-2ε, P8 WT, (A) AP-2ε was expressed in the basal territories in the marginal and intermediate regions of the VNO (segments 1,2,6,7) and at lower levels in the more central basal regions of the VNO (segments 3,4,5, arrow). AP-2ε cells mainly in the basal territories are highlighted by red dotted line (B) Quantification of optic density (OD) indicating differential AP-2ε immunoreactivity in the different regions of the VNO, zone numbers refer to the zones as indicated in (A), each point represents average OD quantifications from independent VNE (A), values normalized to the OD of zone 1. C) Double immunofluorescence against AP-2ε and Gαo on P21 WT shows AP-2ε expression (red) in Gαo positive basal neurons (green, arrowhead). D) Immunohistochemistry against Cre on AP-2εCre KO (P8) shows strong expression of Cre at the marginal and intermediate zones (segments 1,2,6,7) but nearly complete absence of Cre immunodetectability in the medial/central regions of the VNO (zones 3,4,5). In AP-2ε KO Cre immunoreactivity was not limited to cells in the most basal territories, see dotted line, compare to A. E) Quantification of OD indicating different Cre immunoreactivity in the different zones as in (D). F) Immunostaining anti- AP-2ε on AP-2ε KO shows no immunoreactivity, compare to (A). G-G2) Double immunofluorescence on WT against AP-2ε and Ki67 (G-G2), shows lack of AP-2ε expression (red, arrowheads) in proliferating cells (green, arrows). (H-H2) Immunofluorescence against AP-2ε (red, arrowheads) and NeuroD1 (green, arrows) shows lack of colocalization. (I-I2) Immunofluorescence against AP-2ε (red) and Gap43 (green) shows that AP-2ε is expressed in Gap43+ cells (arrows). J-J2) Double immunofluorescence on WT against AP-2ε (red) and Meis2 (green) shows lack of colocalization in the neurogenic niche and a topographic distinction as the VSNs mature and migrate into the medial portions of the VNO (arrows). K) Schematic of the VNO. Zones 1,7 indicate the marginal zones where neurogenesis and differentiation of neurons occur. L) Cartoon summarizing key differentiation steps of VSNs Ascl1+ neural progenitor cells (purple) reside in the progress through maturation stages. AP-2ε immunoreactivity starts after NeuroD1 as Gap43 starts to be expressed. Mature Meis2+ apical (green) and AP-2ε+ basal neurons (red) migrate towards the central zones with increasing expression of olfactory marker protein as they mature (Zone 3–5).

protein expression restricted to post-mitotic cells at a relatively advanced stage of differentiation when Gap43 starts to be expressed and NeuroD1 is no longer immunodetectable (Fig. 1G-I,K,L).

Double immunostaining against AP-2ε and Meis2, which is selectively expressed in apical VSNs (Chang and Parrilla, 2016; Enomoto et al., 2011), revealed complementary/non-overlapping patterns of expression in apical and basal VSNs respectively (Fig. 1J-J2).

3.2. AP-2ε genetic lineage is selective for basal VSNs

In WT animals, AP-2ε protein expression was detected only in putative basal VSNs (Fig. 1 C,J). However, to understand if AP-2ε genetic lineage is exclusive for basal VSNs we took advantage of the Cre inserted in the AP-2ε locus to perform Cre-mediated genetic lineage tracing (Feng et al., 2009). Cre expression in AP-2ε$^{+/-}$ animals overlapped with AP-2ε expression both in the marginal and medial regions

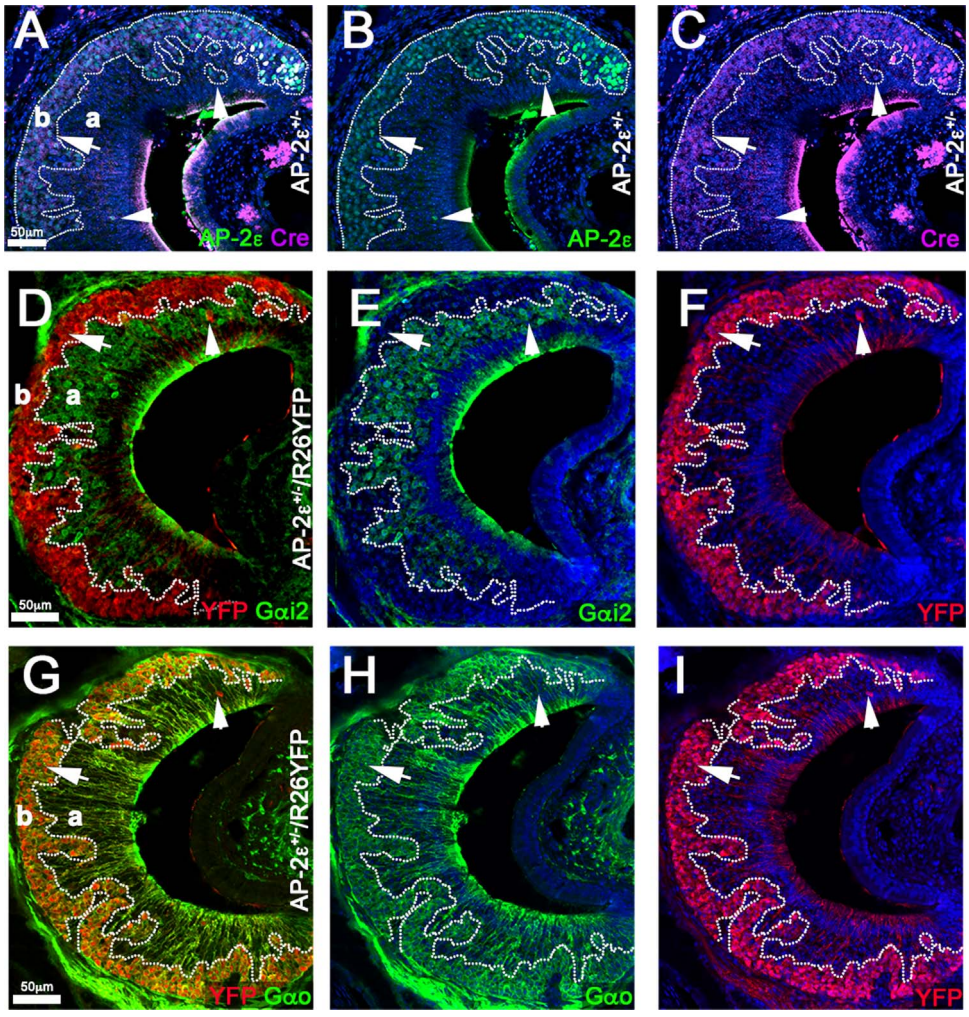

Fig. 2. AP-2ε lineage is selective for basal vomeronasal sensory neurons in the vomeronasal organ. A-C) AP-2ε/Cre double immunostaining on P15 AP-2ε$^{+/-}$, AP-2ε (green, B) and Cre (magenta, C) show overlapping AP-2ε and Cre expression in the basal regions of the VNO (arrow). Few cells positive for both AP-2ε and Cre were found in the apical region (arrowhead). D-F) Double immunostaining on P15 postnatal AP-2εCre$^{+/-}$/R26YFP VNOs against YFP (red) and Gαi2(green). YFP (red) shows AP-2εCre lineage in the basal (b) territories of the VNO (a) but not in the apical (a) cells expressing Gαi2 (green). Arrowhead points to a single neuron positive for AP-2ε in apical region. (G-I) Double immunostaining against YFP (red) and Gαo (green) shows co-localization between AP-2εCre lineage reporter and the basal (b) cell marker Gαo. Arrowhead indicates a single neuron positive for AP-2ε tracing negative for basal marker.

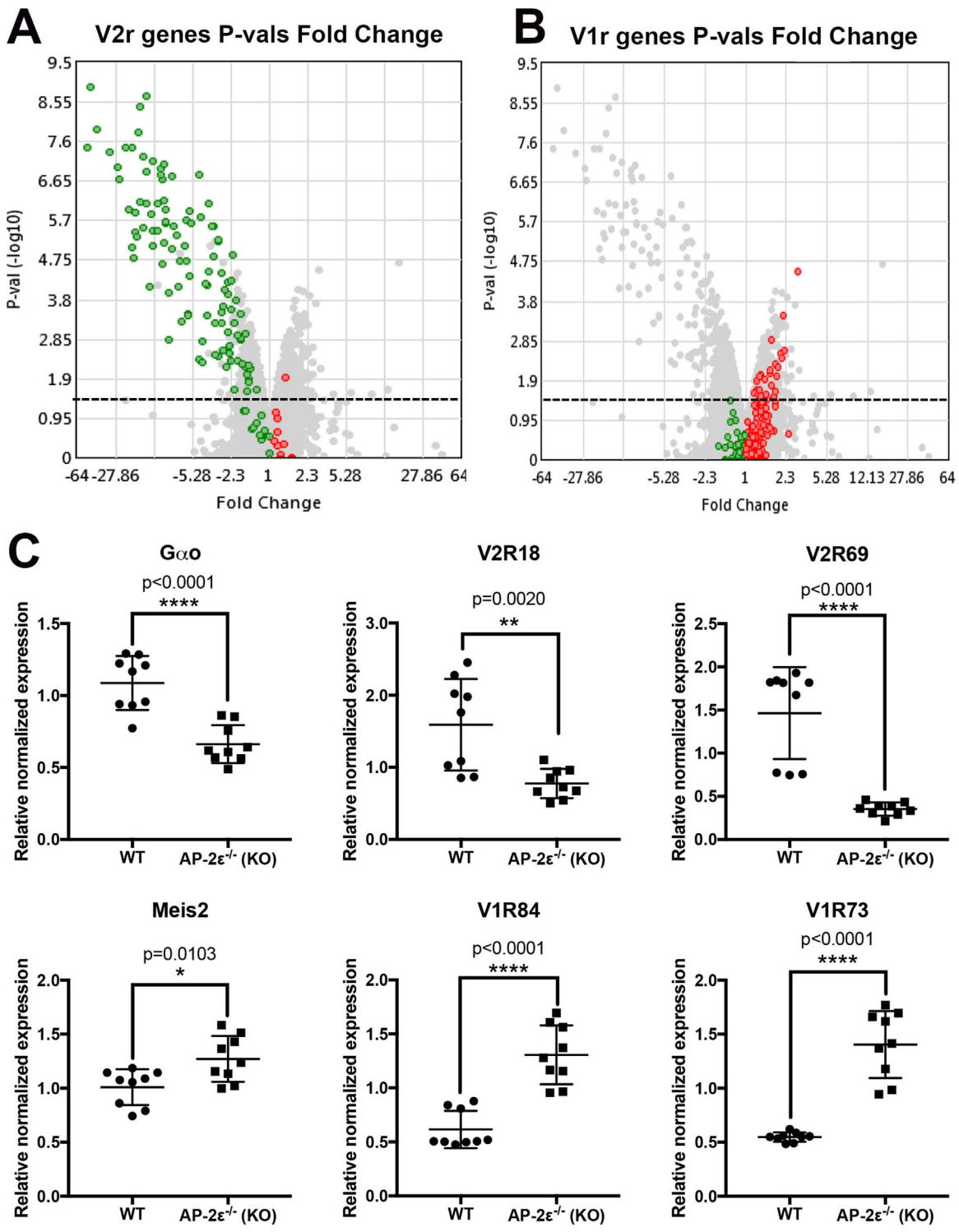

Fig. 3. Microarray data and qRT-PCR data. Affymetrix Mouse Gene ST 2.0 microarray data (WT n = 3; KO n = 3). Volcano plot of V2r (A) and V1r (B) vomeronasal receptor genes expression. Individual vomeronasal receptor genes are plotted against the negative $\log_{10}$ of the adjusted P-value ($-\log_{10}(p = 0.05) = 1.30$; dashed line) against the fold change. All the genes other than V1r and V2rs are represented in gray. All values with a fold change < -1.1 are indicated in green and considered to be significantly down-regulated if $p < 0.05$ while genes with a fold change > 1.1 (red) and considered to be significantly up-regulated. Of the 134 V2r receptors genes expressed, 75% were found to be significantly down-regulated. Of the 213 V1r receptor genes expressed, 5% were found to be significantly upregulated. C) qRT-PCR indicates a decrease in expression for basal markers Gαo ($p < 0.0001$), Vmn2r receptors in AP-2ε null mice together with a significant increase of expression for the apical transcription factor Meis2 and Vmn1rs receptors. Gene expression was normalized to Gapdh before statistical analysis by two-tailed, unpaired *t*-test.

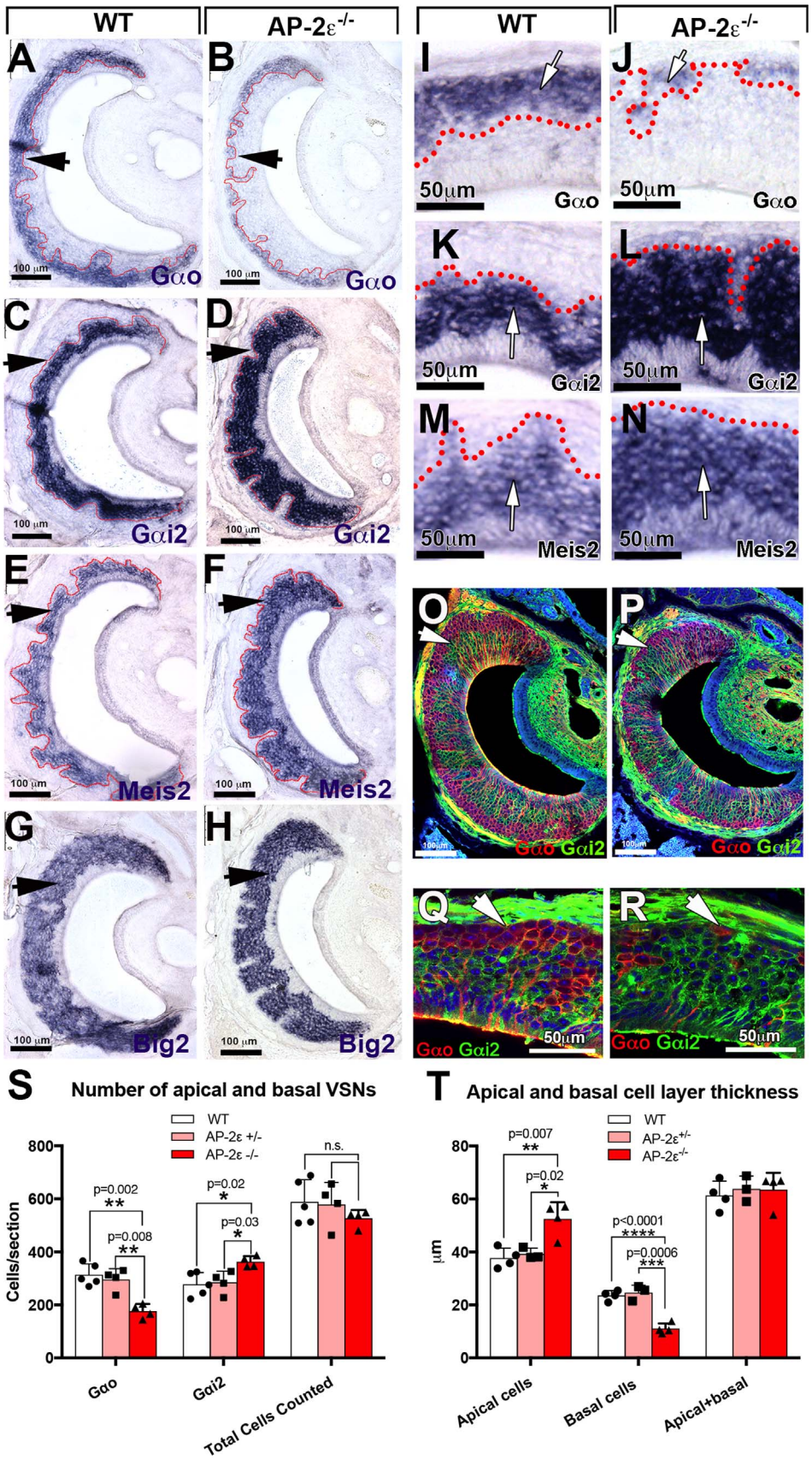
WT
AP-2ε-/-
A
B
Gαo
C
D
Gαi2
E
F
Meis2
G
H
Big2
100 μm
WT
AP-2ε-/-
I
J
K
L
M
N
50μm
Gαo
Gαi2
Meis2
O
P
Gαo Gαi2
Q
R
S
Number of apical and basal VSNs
WT
AP-2ε +/-
AP-2ε -/-
Cells/section
p=0.002
p=0.008
p=0.02
p=0.03
n.s.
Gαo
Gαi2
Total Cells Counted
T
Apical and basal cell layer thickness
WT
AP-2ε+/-
AP-2ε-/-
μm
p=0.007
p=0.02
p<0.0001
p=0.0006
Apical cells
Basal cells
Apical+basal

Fig. 4. AP-2ε loss-of-function disrupts basal vomeronasal sensory neuron development. A-B) In situ hybridization against Gαo on A) WT shows robust Gαo expression (red dotted line) in the basal portion of the VNE. B) AP-2ε KO displays a marked reduction of neuroepithelium positive for Gαo mRNA expression in comparison to WT (black arrow), I,J) High magnification images of Gαo ISH on I) WT and J) AP-2ε KO. C-D) ISH against Gαi2 on C) WT VNO shows the Gαi2 expression (red dotted line) in the apical portion of the neuroepithelium. In the AP-2ε KO, an apparent expansion of the Gαi2 expressing area (black arrow) was observed when compared to WT. O,P) High magnification images of Gαi2 ISH on O) WT and P) KO. E-H) Double immunofluorescence against Gαo (red) and Gαi2 (green) on WT (E,G) display a comparable number of basal and apical VSNs in the neuroepithelium. In the AP-2ε KO (F,H) a significant reduction of the Gαo+ basal population (white arrows) and apparent expansion of the Gαi2+ apical population. ISH against I-J) Meis2 shows a similar expression to Gαi2 in the apical portion of the I) WT vomeronasal epithelium. J) In the AP-2ε KO we observe a similar expansion of Meis2 expression, Q, R) high magnification images of Q) WT and R) AP-2ε KO. ISH against K,L) Big2, which is expressed throughout the vomeronasal epithelium, shows comparable maintained expression between K) WT and L) AP-2ε KO mice. S) Quantifications of average number of Gαo+, Gαi2+, and total number of VSNs in the neuroepithelium of P21 WT and AP-2ε KO mice. In the AP-2ε KO, a significant decrease in the number of Gαo+ basal neurons ($p = 0.009$) and increase in the number of Gαi2+ apical neurons ($p = 0.0008$), with no change in total number of VSNs per section ($p = 0.2$). T) Quantifications of apical, basal, and total neuroepithelium thickness (μm) in P21 WT and AP-2ε KO VNE similarly show significant decrease in the average neuroepithelium thickness of the basal VSN population ($p < 0.0001$) and an increase in the apical population of VSNs ($p = 0.006$), with no significant difference in total epithelium thicknesses. Statistical analysis by two-tailed, unpaired *t*-test.

of the VNO (Fig. 2A-C).

AP-2ε$^{+/-}$/Rosa26R lineage tracing combined with Gαo and Gαi2 immunostaining revealed that AP-2ε is expressed by cells that acquire basal identity (Fig. 2D-I). Quantifications revealed that in AP-2ε$^{+/-}$/Rosa26R, which have one AP-2ε functional allele, 98.8% SE ± 0.1% of the cells positive for AP-2ε lineage expressed Gαo (Fig. 2D-I).

3.3. AP-2ε loss-of-function negatively impacts the development of basal VSNs

Whole transcript analysis of genetic material obtained from dissected VNO from P17 WT and AP-2ε$^{-/-}$ (n = 3;3) was performed via comparative hybridization using Affymetrix Mouse Gene ST 2.0 microarrays. Raw microarray data are available in GEO (GSE110083). Data analysis indicated that loss of AP-2ε leads to a downregulation of virtually all V2r genes (Fig. 3A) and to a significant increase for several V1r genes (Fig. 3B). In addition, the non-classical MHC class I (H2-Mv) genes, which are only expressed by specific basal VSNs subpopulations (Leinders-Zufall et al., 2014), were found to be significantly downregulated (Supplementary, Table S1). Gαo transcripts, which are normally expressed by basal neurons, were significantly decreased by 1.5-fold ($p = 0.01$) while the apical transcription factor Meis2 appeared to be upregulated by 1.25-fold ($p = 0.04$) however, microarray analysis did not show statistically significant changes in Gαi2 expression. The high-throughput data suggested a downregulation of basal markers together with a disparate upregulation of apical genes. Bcl11b mRNA expression levels were not significant between genotypes (data not shown).

These microarray data partially overlapped with gene expression data previously described after *Bcl11b* loss-of-function (Enomoto et al., 2011), where loss of AP-2ε expression, basal markers together with an increase in the early apical marker Meis2 was also observed. This suggested to further explore the impact of AP-2ε in controlling the basal terminal differentiation.

qRT-PCR analysis confirmed a reduction in expression of basal marker Gαo ($p < 0.0001$), V2R receptors, and increase in expression in the apical specific transcription factor Meis2 ($p = 0.01$) and of V1R receptors (Fig. 3C), however Gαi2 expression increase resulted to be the more variable between samples and therefore non-significant (data not shown).

We performed in-situ hybridization (ISH) against the basal marker Gαo, the apical markers Gαi2, Meis2, and against the pan VSN marker Big2 (Enomoto et al., 2011), on WT controls, and AP-2ε KOs (P21, n = 3;3) (Fig. 4A-N). In control animals, the basal marker Gαo was expressed in the basal half of the VNE (Fig. 4A,I) whereas the apical markers Gαi2 and Meis2, were found distributed in the cells in the most apical half of the epithelium (Fig. 4C,E,K,M). However, in AP-2ε null mice, Gαo expression was found to be reduced (Fig. 4 B,J) in the basal territories of the VNE while Gαi2 and Meis2 expression covered most of the epithelium with an expression pattern comparable to the pan VSN marker, Big2 (Fig. 4 D,F-H,K-N).

We also verified the protein expression of basal and apical markers, Gαo and Gαi2, via immunofluorescence (I.F.) which confirmed a dramatic reduction in cells expressing the former basal marker (Fig. 4O-R). Quantifications of the neuroepithelium after Gαo and Gαi2 double immunostaining on WT (AP-2ε$^{+/+}$), AP-2ε$^{+/-}$, and AP-2ε$^{-/-}$ (P21) indicated an overall 11% average reduction, though non-significant ($p = 0.2$), in the total number of cells in the KO. However, a significant decrease in the number of cells expressing the basal markers together with a small increase in the number of neurons expressing apical proteins was observed in the KOs (Fig. 4S,T). No significant differences in apical and basal marker expression were observed between AP-2ε$^{+/+}$ and AP-2ε$^{+/-}$ (Fig. 4S,T).

3.4. Lack of functional AP-2ε can lead to a shift of maturing basal VSNs to the apical differentiation program

Performing double immunostaining against AP-2ε and the apical transcription factor Meis2 (Enomoto et al., 2011) in P21 WT (Fig. 1J-J2, Fig. 5A-A2) or against Cre and Meis2 in P21 AP-2ε$^{-/-}$ (Fig. 5B-B2), we observed that in both conditions the expression of AP-2ε or Cre (in the KO) and Meis2 appeared to be mutually exclusive (Fig. 5A). This indicated that the basal program and apical differentiation program are initiated prior to, and independently from, AP-2ε expression.

However, while in controls the basal neurons retained AP-2ε expression and lacked Meis2 immunoreactivity (Fig. 5A). In AP-2ε KOs Cre expression was found in cells scattered, throughout the apical-basal regions (Fig. 5A-A2), and to be progressively lost while Meis2 expression appears to expand to cells in the basal territories (Fig. 5B).

These data suggest that: 1) AP-2ε expression might be autoregulated and; 2) AP-2ε might have a role in silencing apical specific genes in maturing neurons. However, in AP-2ε$^{-/-}$ mice several basal VSNs, though negative for Cre expression, were still negative for Meis2 (Fig. 5B). These data suggest that part of the basal VSNs can acquire and maintain basal identity independently from AP-2ε expression.

3.5. AP-2εCre/R26R lineage tracing indicates that the apical transcription factor Meis2 is expressed in cells that previously entered the basal program

AP-2εCre$^{+/-}$/R26R lineage tracing combined with Meis2 immunostaining at P21 revealed that in AP-2ε heterozygous animals cells belonging to the AP-2ε lineage, were occasionally positive (1.4% SE ± 0.15, n = 4) for the apical marker Meis2 (Fig. 5C-C2). However, in AP-2ε$^{-/-}$ mice a significantly higher percentage (11.9%, SE ± 1.0, $p = 0.03$, n = 4) of all the traced cells in the VNO were positive for Meis2 expression, and notably these cells were found in both apical and basal territories of the VNO (Fig. 5D-D2).

To understand if the cells that deviated from the basal program to apical can reach maturity we performed a triple immunostaining against the AP-2εCre/R26 lineage tracing, Meis2, and the olfactory marker protein OMP, which is expressed in mature VSNs on P21 KO and control mice. The results indicate that in the KO the Meis2+ cells positive for AP-2ε lineage arrive to express the maturation marker OMP (Fig. 5E-F3).

To test if the cells that appear to switch from the basal to apical

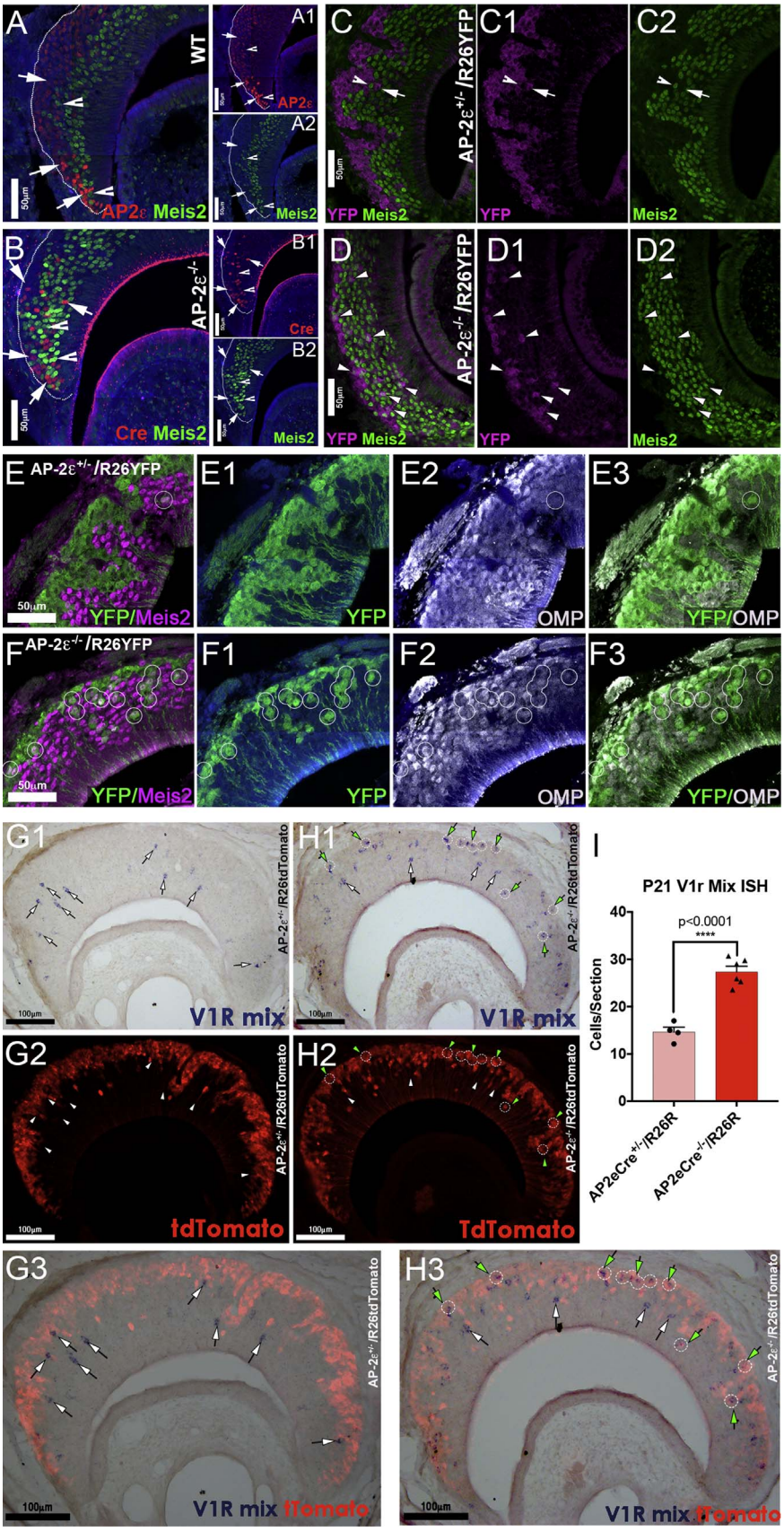
A
WT
AP2ε Meis2
A1
AP2ε
A2
Meis2
C
AP-2ε+/-/R26YFP
YFP Meis2
C1
YFP
C2
Meis2
B
AP-2ε-/-
Cre Meis2
B1
Cre
B2
Meis2
D
AP-2ε-/-/R26YFP
YFP Meis2
D1
YFP
D2
Meis2
E AP-2ε+/-/R26YFP
YFP/Meis2
E1
YFP
E2
OMP
E3
YFP/OMP
F AP-2ε-/-/R26YFP
YFP/Meis2
F1
YFP
F2
OMP
F3
YFP/OMP
G1
AP-2ε+/-/R26tdTomato
V1R mix
H1
AP-2ε-/-/R26tdTomato
V1R mix
I
P21 V1r Mix ISH
p<0.0001
****
Cells/Section
AP2eCre+/-/R26R
AP2eCre-/-/R26R
G2
tdTomato
H2
TdTomato
G3
V1R mix tTomato
H3
V1R mix tTomato

Fig. 5. AP-2ε lineage tracing indicate that cells positive for the AP-2ε/basal lineage can differentiate in apical neurons. A) Double immunofluorescence against AP-2ε (red) and Meis2 (green) on P21 WT shows that AP-2ε and Meis2 do not colocalize in newly generated post-mitotic cells (notched arrows) and that their expression remains mutually exclusive in mature neurons located medially in the VNE (white arrows). B) Double immunofluorescence against Cre (red) and Meis2 (green) on P21 AP-2ε$^{-/-}$ show no colocalization between the two transcription factors (notched arrows). In WT mice, AP-2ε expression persists in mature basal VSNs, while in AP-2ε null mice Cre immunodetectability declines in more medial regions and can be found in interspersed in basal and apical regions of the VNE when compared to controls (white arrows) while the region of Meis2+ cells appears to increase. C,D) Double immunofluorescence against AP-2ε lineage tracing (magenta) and Meis2 (green) on P21 C) AP-2ε$^{+/-}$/R26R^{YFP} and D) AP-2ε$^{-/-}$/R26R^{YFP}. D) In AP-2ε$^{-/-}$ mutants numerous AP-2ε lineage traced cells express Meis2 in both apical and basal regions (arrowheads). E-F3) Triple immunostaining against Meis2 (magenta), YFP(green) and OMP(white) on E-E3) AP-2ε$^{+/-}$/R26R^{YFP} and F-F3) AP-2ε$^{-/-}$/R26R^{YFP}. Cells positive for AP-2ε lineage and Meis2 expression express were found to be also positive for OMP, cells positive for the three markers have been circled to facilitate the identification. G1-H3) P21, in situ hybridization of mix of V1rs (blue) and AP-2ε lineage tracing (red) on AP-2ε$^{+/-}$/R26^{tdTomato} (G1–3) and AP-2ε$^{-/-}$/R26^{tdTomato} (H1–3). V1r+ cells in the apical regions of the VNE negative for AP-2ε lineage tracing are indicated with white arrows. V1r+ cells distributed in the basal region of the VNE (green arrows). Overlaid images (G3,H3), show V1r+ expression in AP-2ε lineage traced cells (white circles) in the KOs but not the controls. I) Significant increase in the total number of V1r expressing cells were observed in the KOs when compared to controls ($p < 0.0003$).

program can express V1r genes, we performed in situ hybridizations against a mix of select V1rs that we found to be consistently increased in the KOs; Vmn1r73 (+2.71 fold p = 0.002), Vmn1r81 (+ 2.04 fold p = 0.04), Vmn1r82(+1.82 fold p = 0.049), and Vmn1r84 (+ 2.13 fold p = 0.044) (Fig. 5 G1,H1,I). In line with the transcriptome data (Fig. 3) we observed a significant increase in the number of cells that express these V1r receptors in AP-2ε$^{-/-}$ mice when compared to controls. Moreover, we observed that in the KO, a large portion of the V1r+ cells were distributed in the basal domain and appeared, as for Meis2 (Fig. 5C,D), to colocalize with AP-2ε lineage tracing (Fig. 5G-H3).

3.6. Cell loss and compensatory proliferation

The VNO undergoes massive neurogenesis in the first ten days after birth which then decreases to maintenance levels as the VNO reaches its final cell number (Wakabayashi and Ichikawa, 2007). AP-2ε is only expressed in post-mitotic cells in the VNO (Fig. 1).

We analyzed proliferation and cell death at two postnatal stages: P8 and P15. Analysis at P8, when the vomeronasal organ is still extensively growing in size and in cell number, revealed significantly higher levels of apoptosis and cell proliferation (Fig. 6A-C,E-G). Notably, we observed that in the KOs the Ki67+ proliferative cells were not limited to the marginal zone, as in controls (Fig. 6A), but also in the intermediate and central regions of the VNO with a pattern suggestive of a compensatory proliferative response due to increased cell loss (Fig. 6B) (Brann and Firestein, 2010; Giacobini et al., 2000). Analysis at P15 also revealed an increase in the number of Ki67+ proliferative cells but non-significant differences in apoptosis (Fig. 6D,H, Fig. S1).

VSNs committed to the apical lineage co-express Gαo and Gαi2 while differentiating and then retain Gαi2 only as they mature (Enomoto et al., 2011). In line with this, we found putative differentiating apical VSNs in the marginal zone positive for both Gαo and Gαi2 (Fig. 6I-J2). Quantifications in controls and AP-2ε null mutants (P21) indicate a significant increase in the number of cells immunoreactive for both Gαo and Gαi2 in the AP-2ε$^{-/-}$ (Fig. 6I, $p < 0.0001$).

3.7. BrdU birth-dating combined with genetic lineage tracing supports that lack of AP-2ε is sufficient for identity shift from basal to apical

Immunolabeling against the V2R family C receptors (V2R2), which is virtually expressed by all basal neurons (Martini et al., 2001), confirmed a reduction in the number of cells expressing basal cell markers in the AP-2ε null animals (Fig. 7A,B,C) as indicated by the microarray (Fig. 3A).

By analyzing V2R2 and Gαo expression on VNO sections of AP-2εCre$^{+/-}$/R26R and AP-2εCre$^{-/-}$/R26R traced animals we found that, while in the controls the basal markers, V2R2 and Gαo, overlap with AP-2ε lineage (Fig. 7E,H,J,L,N), in the KOs there was a significant reduction in the total number of traced cells and in the number of cells positive for AP-2ε tracing and basal markers expression (Fig. 7D,H-O). However, immunostaining against the apical marker Gαi2 and the AP-2ε tracing reporter indicated an increase in cells double positive for AP-2ε tracing and Gαi2 but negative for basal markers (Fig. 6D, H-S).

In order to follow the dynamics of this process we paired AP-2εCre lineage tracing, with BrdU birth dating. BrdU injections were performed on AP-2ε$^{+/-}$/R26^{tdTomato} and AP-2ε$^{-/-}$/ R26^{tdTomato} mice at P7. Samples were collected at P21 (14 days post-injection) to age match with previous observations and cover the reported maturation rate of VSNs in mouse (de la Rosa-Prieto et al., 2010). Despite the increased number of proliferative cells around the time of injection (Fig. 6A-C) quantification of BrdU+ cells 2 weeks after injection indicated a non-significantly higher total number of BrdU+ cells in the KO (Fig. 7E-G). This further suggests a balance between the increased proliferation and apoptosis in P8 AP-2ε null mice (Fig. 6A-C,E-F). However, while in the controls nearly all the BrdU+ cells positive for AP-2ε lineage expressed basal markers V2R2 and Gαo, in the KO only a portion of the newly formed neurons, positive for AP-2ε lineage, were positive for the basal markers (Fig. 7T). Notably, in the KO around 20% of the newly formed cells positive of the AP-2ε lineage express the apical marker Gαi2. These data corroborate that in the absence of functional AP-2ε a larger number of cells positive for AP-2ε lineage access the apical differentiation program.

3.8. AP-2ε is expressed by subsets of mitral cells of the anterior AOB. The phenotype observed in the VNO is cell autonomous

AP-2ε loss of function compromises the organization of mitral cells in the olfactory bulb (OB) (Feng et al., 2009). To understand if the observed phenotypes in the VNO could be secondary to defects in the AOB we monitored AP-2ε expression in the AOB via AP-2ε lineage tracing.

The apical VSNs express Neuropilin-2 (Nrp2) and project to the anterior AOB (a-AOB) while the basal neurons express the guidance receptor Robo2 and project to the posterior AOBs (p-AOB) (Walz et al., 2002; Prince et al., 2009). In mouse, the anterior and posterior glomerular portions of AOB are distinctly separated and are almost equal in size. AP-2εCre lineage tracing at P21 indicated that, in the AOB, the expression of the Rosa reporter was limited to the fibers of the basal VSNs projecting to the glomerular layer of the p-AOB as well as in putative mitral cells in the anterior mitral cell layer (MCL) (Fig. 8A,B,C).

Performing double immunostaining against AP-2ε lineage tracing and the mitral cell marker Tbx21 (Mitsui et al., 2011; Yoshihara et al., 2005) we found that AP-2ε lineage in the MCL, in contrast to the glomerular layer, was limited to subsets of the mitral cells in the anterior AOB, where only the apical neurons project (Fig. 8B-D). Using Tbx21 as mitral cell marker we quantified the average mitral cell numbers in controls and KO mice (Fig. 8E-F,H), indicating no significant effect of AP-2ε loss-of-function on the number of mitral cells.

By analyzing sections of traced AP-2ε$^{+/-}$ controls and AP-2ε$^{-/-}$ (KO) we observed a significant reduction in the posterior glomerular layer of the AOB (Fig. 8B,C,G), which likely reflects the reduced number of basal neurons in the VNO and not defects in the MCL.

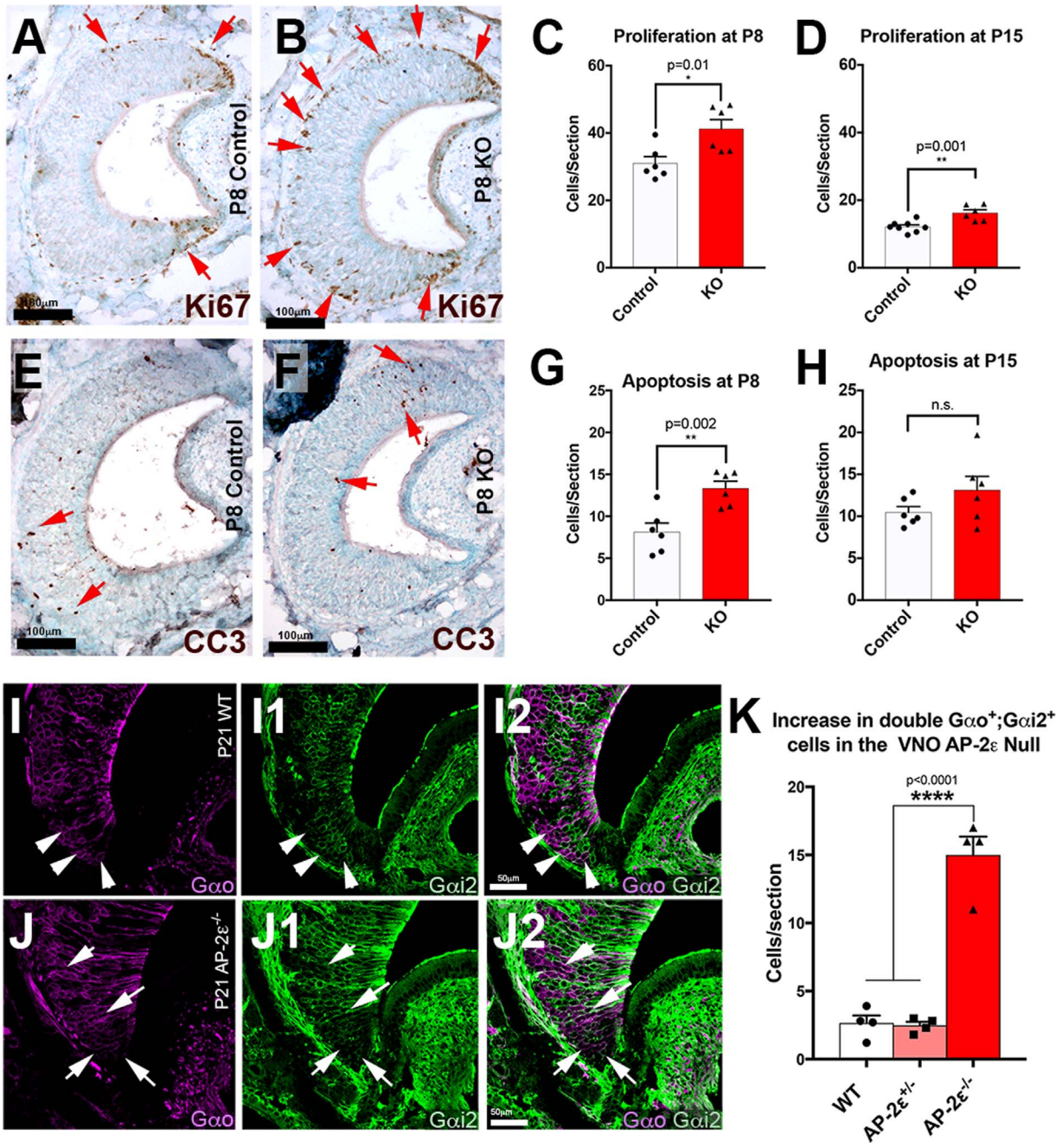

Fig. 6. Immunohistochemistry against the proliferation marker, Ki67 on P8 control (A) show proliferation mainly in the marginal zones, while in the KO (B) we observe an increase in the total number of proliferating cells in addition to more Ki67+ cells in the intermediate and central zones of the VNE. Quantifications of the number of proliferative cells per section in P8 (C) and P15 (D) show a significant increase in the rate of proliferation in the AP-2ε KO mice when compared to controls. Immunohistochemistry against the apoptotic marker, cleaved-caspase-3 (CC3), on P8 control (E) and KO (F). Quantification of CC3+ cells at P8 (G) shows a significant increase in the number of apoptotic cells in KOs when compared to controls. Quantification of CC3+ at P15 (H) revealed a slight but nonsignificant increase in the number of apoptotic cells in KOs when compared to controls. I-J2) Double immunofluorescence against Gαo (magenta) and Gαi2 (green) on P21 AP-2ε I) WT VNOs show the immature VSNs that are positive for both Gαo and Gαi2, however in P21 AP-2ε null animals (J), the average number of these double positive cells significantly increases when compared to both WT and AP-2$\varepsilon^{-/-}$ controls (I, $p < 0.0001$). Statistical analysis by two-tailed, unpaired *t*-test.

4. Discussion

In the last two decades, we have made significant progress in understanding cell composition, axonal guidance, and the molecular basis of chemosensory detection of the VNO (Chamero et al., 2012; Stein et al., 2016). Old or damaged VSNs are constantly replaced by newly formed cells that are incorporated into functional circuits. However, the molecular mechanisms underlying the various steps of differentiation and homeostasis of newborn neurons are not fully understood (Enomoto et al., 2011; Oboti et al., 2015).

Apical and basal VSNs originate from a common pool of progenitor cells, and transiently share common expression of Gαo during the process of differentiation (Enomoto et al., 2011). In normal conditions, apical and basal VSNs are generated at comparable rates and numbers (de la Rosa-Prieto et al., 2010).

Expression of the transcription factor, AP-2ε, has been previously described in the basal cell layer of the VNO and proposed to potentially act downstream of the zinc-finger transcription protein, Bcl11b, to activate the basal VSN differentiation program and neuronal viability (Suarez, 2011), however this has never been further investigated.

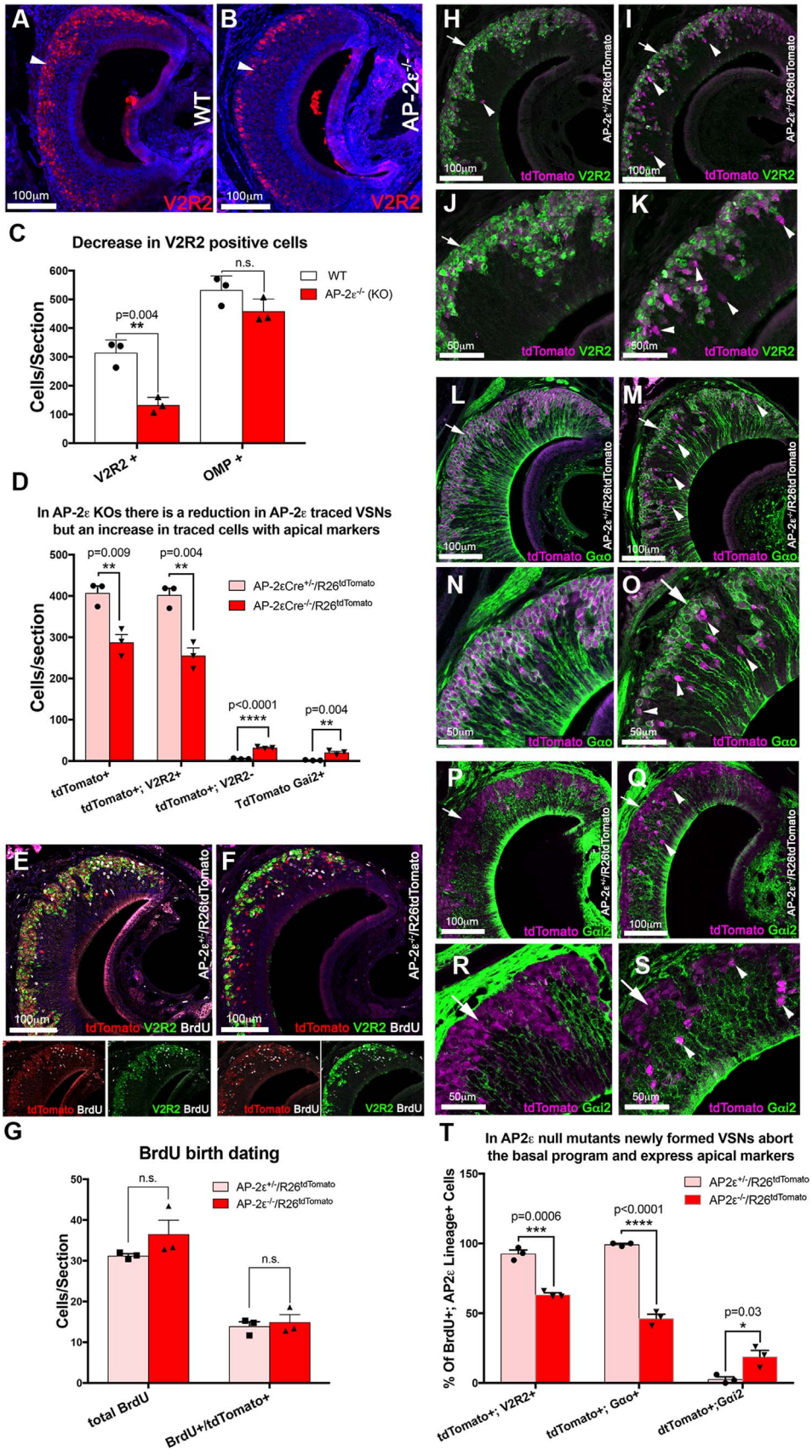
A
WT
V2R2
100μm
B
AP-2ε-/-
V2R2
100μm
C
Decrease in V2R2 positive cells
Cells/Section
WT
AP-2ε-/- (KO)
p=0.004
**
n.s.
V2R2 +
OMP +
D
In AP-2ε KOs there is a reduction in AP-2ε traced VSNs
but an increase in traced cells with apical markers
Cells/section
p=0.009
**
p=0.004
**
p<0.0001
****
p=0.004
**
AP-2εCre+/-/R26tdTomato
AP-2εCre-/-/R26tdTomato
tdTomato+
tdTomato+; V2R2+
tdTomato+; V2R2-
TdTomato Gαi2+
E
F
AP-2ε+/-/R26tdTomato
AP-2ε-/-/R26tdTomato
100μm
tdTomato V2R2 BrdU
tdTomato BrdU
V2R2 BrdU
G
BrdU birth dating
Cells/Section
n.s.
n.s.
AP-2ε+/-/R26tdTomato
AP-2ε-/-/R26tdTomato
total BrdU
BrdU+/tdTomato+
H
I
AP-2ε+/-/R26tdTomato
AP-2ε-/-/R26tdTomato
100μm
tdTomato V2R2
J
K
50μm
tdTomato V2R2
L
M
AP-2ε+/-/R26tdTomato
AP-2ε-/-/R26tdTomato
100μm
tdTomato Gαo
N
O
50μm
tdTomato Gαo
P
Q
AP-2ε+/-/R26tdTomato
AP-2ε-/-/R26tdTomato
100μm
tdTomato Gαi2
R
S
50μm
tdTomato Gαi2
T
In AP2ε null mutants newly formed VSNs abort
the basal program and express apical markers
% Of BrdU+; AP2ε Lineage+ Cells
p=0.0006
***
p<0.0001
****
p=0.03
*
AP2ε+/-/R26tdTomato
AP2ε-/-/R26tdTomato
tdTomato+; V2R2+
tdTomato+; Gαo+
dtTomato+;Gαi2

Fig. 7. AP-2εCre null mice show a higher number of cells positive AP-2ε lineage that acquire apical-like characteristics. A,B) Immunofluorescence against V2R2 (red) on P21 AP-2ε WT (A) and AP-2ε $^{-/-}$ (B) shows a dramatic reduction in the cells positive for V2R2. C) Quantification of number of V2R2+ and OMP cells/section shows a significant reduction in V2R2+ cells in AP-2ε $^{-/-}$ (p = 0.004) but non-significant reduction in the total number of mature VSNs positive for OMP. D) Quantification of total AP-2εCre traced cells, traced cells positive for V2R2 expression and Gαi2 expression in AP-2ε$^{+/-}$/R26^{tdTomato} controls and AP-2ε$^{-/-}$/R26^{tdTomato} (Null). Data show a significant reduction in cells positive for AP-2ε tracing in the KO as well as in the number of cells expressing the basal marker V2R2. In the KO there is a similar significant increase in traced cells negative for V2R2 and in cells expressing the apical marker Gαi2. E-F) Representative image of immunostainings against AP-2ε lineage tracing (tdTomato, red), V2R2 (green), and BrdU (white) at P21 on AP-2ε$^{+/-}$/R26^{tdTomato} (D) and AP-2ε$^{-/-}$/R26^{tdTomato}. G) Quantification of neurons formed 2 weeks after BrdU injection. The number of newly born neurons and the number of BrdU+ AP-2ε lineage traced neurons are similar between AP-2ε$^{+/-}$/R26^{tdTomato} controls and AP-2ε$^{-/-}$ R26^{tdTomato}. H-K) Double immunofluorescence against the Rosa reporter tdTomato (magenta) and V2R2 (green) on P21 AP-2ε$^{+/-}$/R26^{tdTomato} (H,J) show colocalization in the basal region of the epithelium (arrow). Sparse cells positive for AP-2ε lineage negative for V2R2 (arrowheads) were detected in apical region. (I,K) A large number of AP-2ε traced cells (magenta) are negative for V2R2 expression in both basal and apical territories (arrowheads). L-O) Double immunofluorescence against the Rosa reporter tdTomato (magenta) and Gαo (green). L,N) P21 AP-2ε$^{+/-}$/R26^{tdTomato} show tdTomato and Gαo colocalization in the basal region of the epithelium (arrow). (M,O) In AP-2ε null mice a large number of AP-2ε traced cells (magenta) are negative for Gαo expression in both basal and apical territories (arrowheads). P-S) AP-2ε lineage tracing (magenta) and Gαi2 expression (green) in P21 AP-2ε$^{+/-}$/R26^{tdTomato} (P,R) show cells positive for AP-2ε lineage in the basal half of the VNE do not express the apical marker Gαi2 (arrow). (Q,S) AP-2ε$^{-/-}$/R26^{tdTomato} VNE several cells positive for AP-2ε lineage (magenta) are positive for Gαi2 (arrowheads). T) Quantification of BrdU labeled cells 2 weeks after BrdU injection positive AP-2ε lineage, basal markers (V2R and Gαo) and apical marker (Gαi2). Data show a reduction in basal marker expression in the KO (V2R2 + p-0.0005; Gαo, $p < 0.0001$) and a small but a significant increase in the number of BrdU+/lineage traced cells that express the apical marker (Gαi2, p = 0.03). Statistical analysis by two-tailed, unpaired *t*-test.

AP-2ε is one of five members of the activating protein-2 (AP-2) family of transcription factors, which play important roles in embryonic development in a variety of tissues, including the CNS. They are often found in cell type-specific expression in either subsets of neural progenitors or post-mitotic developing neurons, suggesting intrinsic roles in cell type specification, differentiation, and identity maintenance (Bassett et al., 2012; Feng et al., 2009; Hong et al., 2014; Kantarci et al., 2015; Pinto et al., 2009).

By analyzing a line of AP-2ε null mice we found that lack of functional AP-2ε translates into a severe reduction in expression of basal specific genes, including virtually the entire gene family of V2R receptors and Gαo, and to an increase in cells expressing apical markers.

Analysis of proliferation and apoptosis revealed significantly higher cell loss and proliferation in young postnatal animals (P8), when the VNO is growing, however, at P15 we found slightly higher proliferation but not significantly higher apoptosis. Progenitor cells in the marginal zone are largely responsible for growth, while progenitors in the central zone are associated with cell replacement (Brann and Firestein, 2010; Giacobini et al., 2000). The pattern observed in the KO, with proliferative cells in medial and central areas of the VNO suggest that the increased proliferation could be a reaction of the VNE to increased loss of basal cells. This suggests that the comparable size of the VNOs observed at P21, a stage at which the VNO is fully formed (Wakabayashi and Ichikawa, 2007), could, in part, reflect a slow and continuous negative selection of basal neurons and an enrichment in apical cells.

Neuronal differentiation is defined by the activation of specific transcriptional programs that are maintained throughout the life of a cell. By analyzing AP-2ε expression via immunohistochemistry and genetic lineage tracing we found that, in the VNO, AP-2ε is highly expressed in post-mitotic maturing basal neurons and that its expression is retained as the neurons mature (Fig. 1). In line with this, AP-2ε Cre lineage tracing revealed that, in AP-2ε$^{+/-}$ animals, ~ 99% of the cells that expressed AP-2ε acquire basal identity. Moreover, we found that AP-2ε immunodetectability does not overlap with the expression of the transcription factor Meis2, which is expressed in cells committed to become apical neurons (Enomoto et al., 2011) (Figs. 1,5). In AP-2ε null mice we found that also the non-functional AP-2ε (Cre) was expressed in maturing VSNs in the more marginal zones of the VNO with a pattern mutually exclusive with Meis2. These data indicate that: 1) the apical-basal differentiation dichotomy is established prior to and independently of AP-2ε expression and; 2) for at least some of the cells that entered the basal program, suppression of apical markers appears to be independent from functional AP-2ε expression (Fig. 9). Moreover, microarray data confirmed a decrease in expression for most the V2R genes, together with an increase in transcripts for V1R receptors. Additionally, by combining immunolabeling anti Meis2 and ISH against selected V1rs with AP-2ε lineage tracing we found that, without functional AP-2ε, some of the cells that initiated the basal differentiation program can express apical specific genes. OMP immunostaining on traced animals revealed that the cells that transitioned from basal to the apical or apical-like program can reach maturity.

The finding that in the absence of functional AP-2ε some basal VSNs can switch to the apical program was further supported in BrdU birth dating experiments combined with AP-2ε lineage tracing. In fact, 2 weeks post-BrdU injection we found that in AP-2ε null mice, only half of the cells positive for AP-2ε lineage resulted to be positive for basal markers; V2R2 and Gαo.

The process of terminal differentiation begins as soon as the cells exit cell cycle. During differentiation, cells express identity-specific genes that progressively decrease potency and plasticity of the cells as they acquire their identity specification (Patel and Hobert, 2017). We found that AP-2ε expression turns on in post-mitotic cells after the apical-basal dichotomy has been initiated, indicated by the mutually exclusive expression of either AP-2ε or Meis2. These data suggest that AP-2ε has a role in sustaining the expression of basal specific genes once the apical-basal dichotomy is already established.

Our lineage tracing experiments suggest that, in the VNO, some of the cells that already enter the basal differentiation program (up to AP-2ε/Cre expression) still retain a sufficient level of cellular plasticity that allows them to abort this program, and switch to the alternative apical terminal differentiation program. Genetic lineage tracing using AP-2εCre$^{+/-}$ mice, which express only one functional allele of AP-2ε, revealed that even in the presence of functional AP-2ε, around 1% of the basal cells can differentiate into apical VSNs.

This observation suggests different interpretations: 1) that reduced levels of AP-2ε expression might not be sufficient to maintain the basal program after differentiation or 2) that the VSNs always have a long window of plasticity and cells that enter the basal differentiation program can naturally switch to the alternative apical program in response to genetic abnormalities, lack of connectivity, hormonal stimuli, or environmental changes during the process of differentiation.

In AP-2ε null mice we observed a reduction but not complete loss of neurons expressing basal VSNs markers. These data indicate that, even in the absence of AP-2ε, VSNs can initiate, the basal program (Fig. 9). These data also suggest that AP-2ε is needed to maintain basal identity for a large portion of basal VSNs but not essential for all (Fig. 9B). However, our array data indicate that the V2r genes of all families (not shown) as well as the non-classical MHC class I (H2-Mv) genes, which are only expressed by specific basal VSNs subpopulations (Leinders-Zufall et al., 2014, 2009), are reduced in AP-2ε mutants (Table S1) making it difficult to understand what selects the VSNs ability to survive and differentiate without AP-2ε.

Notably, incomplete ablation of basal VSNs has been also observed after loss-of-function of Ascl-1 and Ngn-1 (Cau et al., 2002), G-protein subunit Gγ-8 (Montani et al., 2013), Gαo (Chamero et al., 2011), Retinoic Acid Receptor (Hornberg et al., 2009)and the transcription factor ATF5 (Nakano et al., 2016). What underlies the varying

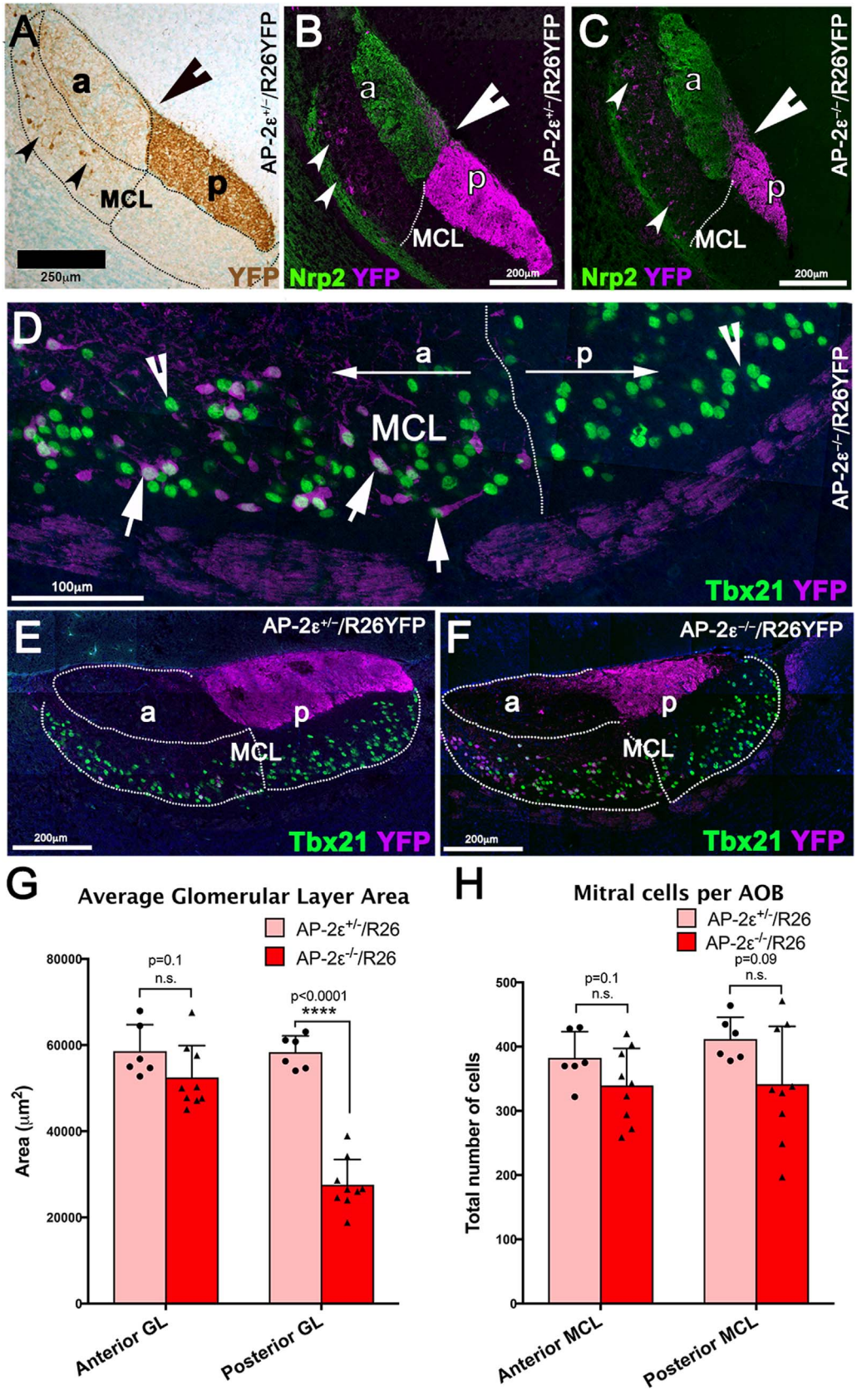
A
a
p
MCL
250μm
YFP
AP-2ε+/−/R26YFP
B
a
p
MCL
200μm
Nrp2 YFP
AP-2ε+/−/R26YFP
C
a
p
MCL
200μm
Nrp2 YFP
AP-2ε−/−/R26YFP
D
a
p
MCL
100μm
Tbx21 YFP
AP-2ε−/−/R26YFP
E
AP-2ε+/−/R26YFP
a
p
MCL
200μm
Tbx21 YFP
F
AP-2ε−/−/R26YFP
a
p
MCL
200μm
Tbx21 YFP
G
Average Glomerular Layer Area
AP-2ε+/−/R26
AP-2ε-/-/R26
p=0.1
n.s.
p<0.0001
****
Area (μm2)
80000
60000
40000
20000
0
Anterior GL
Posterior GL
H
Mitral cells per AOB
AP-2ε+/−/R26
AP-2ε-/-/R26
p=0.1
n.s.
p=0.09
n.s.
Total number of cells
500
400
300
200
100
0
Anterior MCL
Posterior MCL

Fig. 8. The glomerular layer of the posterior accessory olfactory bulb is reduced with no significant changes to the anterior glomerular layer or mitral/tufted cell layers. A) Immunohistochemistry against YFP on parasagittal sections of the AOB of AP-2ε$^{+/-}$/R26YFP (P21) shows the basal vomeronasal fibers projecting to the posterior glomerular layer (GL) of the AOB along with cell bodies in the anterior mitral cell layer (MCL) (black arrow heads) (black notched arrow) but into the posterior MCL (regions traced with black dotted line). B,C) Immunofluorescence against Nrp2 (green) and lineage tracing (magenta) on B) AP-2ε$^{+/-}$/R26YFP and C) AP-2ε$^{-/-}$/R26YFP mice. Axons from the apical neurons (Nrp2+) populate the anterior GL of the AOB in both AP-2ε$^{+/-}$ and AP-2ε null animals. Traced fibers from the VNO defasciculate at the border between the anterior AOB (a-AOB) and posterior AOB (p-AOB) (notched arrow). C) Reduced posterior (p) GL was observed in AP-2ε null mice compared to controls (B), see quantification in (G). D) Immunostaining against the mitral cell marker, Tbx21 (green), and the R26 marker YFP (magenta). Tbx21+ mitral cells negative for the AP-2ε lineage (notched arrow) were found throughout the anterior and posterior MCL, however a subpopulation of mitral cells was observed to be positive for the AP-2ε lineage tracing (white arrows), but was restricted to the anterior portion of the MCL, (a-MCL and p-MCL marked separated by white dotted line). E,F) Immunostaining against the mitral cell marker, Tbx21 (green) and YFP (magenta) on AOBs of AP-2ε$^{+/-}$/R26YFP (E) and AP-2ε$^{-/-}$/R26YFP (F) show Tbx21+ mitral cells throughout the anterior and posterior MCL in both genotypes (quantification in H). G) Quantification of the average area of GL of the AOB in AP-2ε$^{+/-}$/R26YFP and AP-2ε$^{-/-}$/R26YFP shows non-significant difference in the a-AOB between genotypes ($p = 0.1$), but significant reduction in p-AOB of AP-2εKO ($p < 0.0001$). H) Quantifications of the total number of Tbx21+ cells in the MCL of AP-2ε$^{+/-}$/R26YFP and AP-2ε$^{-/-}$/R26YFP showed non-significant decrease in the posterior MCL ($p = 0.09$). Statistical analysis by two-tailed, unpaired *t*-test.

responses and potential compensatory mechanisms to these mutations requires further investigation.

AP-2ε lineage tracing on AP-2ε$^{+/-}$ and AP-2ε$^{-/-}$ showed a reduced posterior AOB which, as expected, reflects the smaller number of axons projecting in the posterior AOB. However, AP-2ε is also expressed by second order olfactory neurons such as the mitral/tufted cells of the main and accessory olfactory bulb. AP-2ε loss-of-function affects normal olfactory bulb cell organization (Feng et al., 2009). The cells of the aAOB and pAOB have different origins (Huilgol et al., 2013). The mitral cells of the aAOB, as those ones of the main olfactory bulb, emerge from the rostral end of the telencephalon whereas the cells of the pAOB arise from the thalamic eminence at the diencephalic-telencephalic boundary (Huilgol et al., 2013).

Our data show that, in the AOB, AP-2ε genetic lineage tracing is limited to the mitral cells of the anterior AOB, where the apical VSNs, negative for AP-2ε lineage, project. Moreover, the AP-2ε loss-of-function seem to have no effect on the total number of mitral cells in the AOB. These data support a similar lineage for the mitral cells of the aAOB to the ones of the main olfactory bulb and further suggest that the observed phenotypes in the basal VNE are cell autonomous rather than secondary to defects in the pAOB.

In conclusion (Fig. 9), this work demonstrated, for the first time, that AP-2ε is expressed in post-mitotic cells of the VNO and that this transcription factor is not required for initiating the apico-basal dichotomy, but is a crucial molecular player in the maintenance of the basal differentiation program. Our data suggest that AP-2ε expression in VSNs is self-maintained (Fig. 1) and suggests a role for this transcription factor in maintaining basal genes' expression and in preventing the activation of genes belonging to the apical genetic program. Key questions that need to be answered in follow-up studies are; what initiates the apical-basal dichotomy? What are the AP-2ε direct gene targets and binding partners, and what epigenetic modifications occur after AP-2ε expression during the VSNs differentiation process?

Furthermore, the early establishment the basal program suggests the existence of unknown external regulatory inputs (e.g. juxtacrine, paracrine inductive signals) influencing terminal differentiation and cellular plasticity prior to AP-2ε expression.

Further defining the inductive signals and the gene regulatory networks governing AP-2ε expression and VSN differentiation will provide important insights concerning neuronal cellular plasticity, adaptation, and tuning of chemosensory epithelia to hormones (Oboti et al., 2015), experience (Xu et al., 2016) and environmental stimuli.

Acknowledgements

This work was supported by SUNY startups funds.

We thank Dr. T. Williams (Department of Craniofacial Biology, University of Colorado) for sharing the AP-2εCre mouse line. We thank Dr. J.F. Cloutier for providing plasmids to generate probes against Gαo and Gαi2. We thank Dr. R. Tirindelli (Parma University, Italy) for providing the V2R2 antibody. We also thank Dr. T. Williams, Dr. J.F. Cloutier, and Dr. R. Tirindelli additionally for their critical reading of the manuscript.

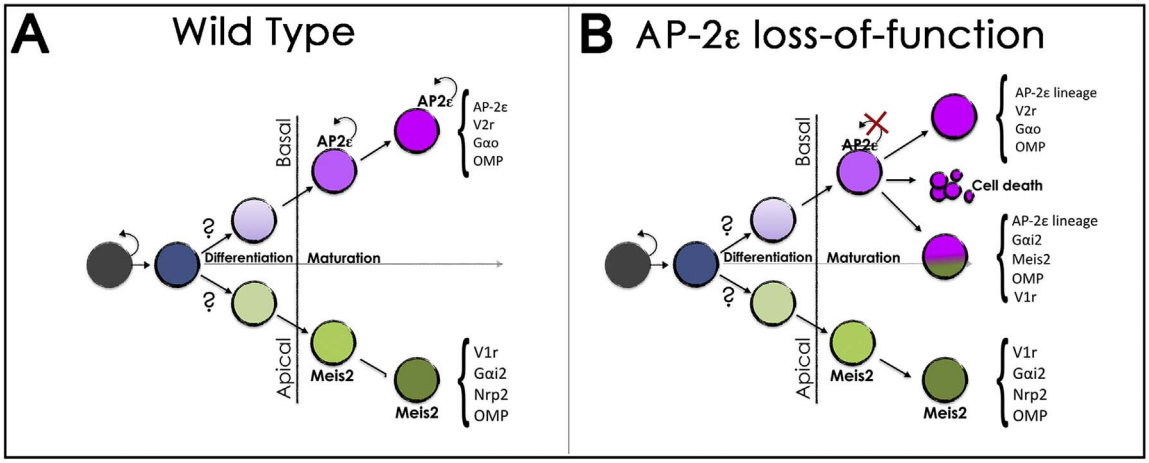

Fig. 9. Summary of AP-2ε effect on VSNs identity maintenance after terminal differentiation. A) Early post-mitotic neurons (Blue) are directed by still unknown (?) signals, to initiate either the basal (purple- > magenta) or apical (green) differentiation programs. Differentiated neurons will express either AP-2ε (basal transcription factor) or Meis2 (apical transcription factor). In wild type animals AP-2ε expression appears to be self-sustained in differentiated basal cells expressing basal markers (listed in brackets). B) In the absence of AP-2ε the apical-basal dichotomy is still established as, in the KOs, Cre (nonfunctional AP-2ε) and Meis2 are still expressed in a mutually exclusive fashion (See Fig. 5), however nonfunctional AP-2ε cannot sustain its own expression (see Fig. 1). In the absence of functional AP-2ε some of the basal VSNs retain basal gene expression, some undergo apoptosis while some express apical markers, this suggests that VSNs can transdifferentiate to apical after the basal differentiation program has been established.

Appendix A. Supporting information

Supplementary data associated with this article can be found in the online version at doi:10.1016/j.ydbio.2018.06.007.

References

Bassett, E.A., Korol, A., Deschamps, P.A., Buettner, R., Wallace, V.A., Williams, T., West-Mays, J.A., 2012. Overlapping expression patterns and redundant roles for AP-2 transcription factors in the developing mammalian retina. Dev. Dyn.: Off. Publ. Am. Assoc. Anat. 241, 814–829.

Brann, J.H., Firestein, S., 2010. Regeneration of new neurons is preserved in aged vomeronasal epithelia. J. Neurosci. 30, 15686–15694.

Cau, E., Casarosa, S., Guillemot, F., 2002. Mash1 and Ngn1control distinct steps of determination and differentiation in the olfactory sensory neuron lineage. Development 129, 1871–1880.

Cau, E., Gradwohl, G., Fode, C., Guillemot, F., 1997. Mash1 activates a cascade of bHLH regulators in olfactory neuron progenitors. Development 124, 1611–1621.

Chamero, P., Katsoulidou, V., Hendrix, P., Bufe, B., Roberts, R., Matsunami, H., Abramowitz, J., Birnbaumer, L., Zufall, F., Leinders-Zufall, T., 2011. G protein G(alpha)o is essential for vomeronasal function and aggressive behavior in mice. Proc. Natl. Acad. Sci. USA 108, 12898–12903.

Chamero, P., Leinders-Zufall, T., Zufall, F., 2012. From genes to social communication: molecular sensing by the vomeronasal organ. Trends Neurosci. 35, 597–606.

Chang, I., Parrilla, M., 2016. Expression patterns of homeobox genes in the mouse vomeronasal organ at postnatal stages. Gene Expr. Patterns 21, 69–80.

Cloutier, J.F., Sahay, A., Chang, E.C., Tessier-Lavigne, M., Dulac, C., Kolodkin, A.L., Ginty, D.D., 2004. Differential requirements for semaphorin 3F and Slit-1 in axonal targeting, fasciculation, and segregation of olfactory sensory neuron projections. J. Neurosci. 24, 9087–9096.

de la Rosa-Prieto, C., Saiz-Sanchez, D., Ubeda-Banon, I., Argandona-Palacios, L., Garcia-Munozguren, S., Martinez-Marcos, A., 2010. Neurogenesis in subclasses of vomeronasal sensory neurons in adult mice. Dev. Neurobiol. 70, 961–970.

Dulac, C., Axel, R., 1995. A novel family of genes encoding putative pheromone receptors in mammals. Cell 83, 195–206.

Enomoto, T., Ohmoto, M., Iwata, T., Uno, A., Saitou, M., Yamaguchi, T., Kominami, R., Matsumoto, I., Hirota, J., 2011. Bcl11b/Ctip2 controls the differentiation of vomeronasal sensory neurons in mice. J. Neurosci. 31, 10159–10173.

Feng, W., Simoes-de-Souza, F., Finger, T.E., Restrepo, D., Williams, T., 2009. Disorganized olfactory bulb lamination in mice deficient for transcription factor AP-2epsilon. Mol. Cell. Neurosci. 42, 161–171.

Forni, P.E., Fornaro, M., Guenette, S., Wray, S., 2011. A role for FE65 in controlling GnRH-1 neurogenesis. J. Neurosci. 31, 480–491.

Forni, P.E., Scuoppo, C., Imayoshi, I., Taulli, R., Dastru, W., Sala, V., Betz, U.A., Muzzi, P., Martinuzzi, D., Vercelli, A.E., Kageyama, R., Ponzetto, C., 2006. High levels of Cre expression in neuronal progenitors cause defects in brain development leading to microencephaly and hydrocephaly. J. Neurosci. 26, 9593–9602.

Giacobini, P., Benedetto, A., Tirindelli, R., Fasolo, A., 2000. Proliferation and migration of receptor neurons in the vomeronasal organ of the adult mouse. Brain Res. Dev. Brain Res. 123, 33–40.

Herrada, G., Dulac, C., 1997. A novel family of putative pheromone receptors in mammals with a topographically organized and sexually dimorphic distribution. Cell 90, 763–773.

Hobert, O., 2016. Terminal selectors of neuronal identity. Curr. Top. Dev. Biol. 116, 455–475.

Hong, C.S., Devotta, A., Lee, Y.H., Park, B.Y., Saint-Jeannet, J.P., 2014. Transcription factor AP2 epsilon (Tfap2e) regulates neural crest specification in Xenopus. Dev. Neurobiol. 74, 894–906.

Hornberg, M., Gussing, F., Berghard, A., Bohm, S., 2009. Retinoic acid selectively inhibits death of basal vomeronasal neurons during late stage of neural circuit formation. J. Neurochem. 110, 1263–1275.

Huilgol, D., Udin, S., Shimogori, T., Saha, B., Roy, A., Aizawa, S., Hevner, R.F., Meyer, G., Ohshima, T., Pleasure, S.J., Zhao, Y., Tole, S., 2013. Dual origins of the mammalian accessory olfactory bulb revealed by an evolutionarily conserved migratory stream. Nat. Neurosci. 16, 157–165.

Kantarci, H., Edlund, R.K., Groves, A.K., Riley, B.B., 2015. Tfap2a promotes specification and maturation of neurons in the inner ear through modulation of Bmp, Fgf and notch signaling. PLoS Genet. 11, e1005037.

Leinders-Zufall, T., Ishii, T., Chamero, P., Hendrix, P., Oboti, L., Schmid, A., Kircher, S., Pyrski, M., Akiyoshi, S., Khan, M., Vaes, E., Zufall, F., Mombaerts, P., 2014. A family of nonclassical class I MHC genes contributes to ultrasensitive chemodetection by mouse vomeronasal sensory neurons. J. Neurosci. 34, 5121–5133.

Leinders-Zufall, T., Ishii, T., Mombaerts, P., Zufall, F., Boehm, T., 2009. Structural requirements for the activation of vomeronasal sensory neurons by MHC peptides. Nat. Neurosci. 12, 1551–1558.

Madisen, L., Zwingman, T.A., Sunkin, S.M., Oh, S.W., Zariwala, H.A., Gu, H., Ng, L.L., Palmiter, R.D., Hawrylycz, M.J., Jones, A.R., Lein, E.S., Zeng, H., 2010. A robust and high-throughput Cre reporting and characterization system for the whole mouse brain. Nat. Neurosci. 13, 133–140.

Martinez-Marcos, A., Ubeda-Banon, I., Halpern, M., 2000. Cell turnover in the vomeronasal epithelium: evidence for differential migration and maturation of subclasses of vomeronasal neurons in the adult opossum. J. Neurobiol. 43, 50–63.

Martini, S., Silvotti, L., Shirazi, A., Ryba, N.J., Tirindelli, R., 2001. Co-expression of putative pheromone receptors in the sensory neurons of the vomeronasal organ. J. Neurosci. 21, 843–848.

Matsunami, H., Buck, L.B., 1997. A multigene family encoding a diverse array of putative pheromone receptors in mammals. Cell 90, 775–784.

Mitsui, S., Igarashi, K.M., Mori, K., Yoshihara, Y., 2011. Genetic visualization of the secondary olfactory pathway in Tbx21 transgenic mice. Neural Syst. Circuits 1, 5.

Montani, G., Tonelli, S., Sanghez, V., Ferrari, P.F., Palanza, P., Zimmer, A., Tirindelli, R., 2013. Aggressive behaviour and physiological responses to pheromones are strongly impaired in mice deficient for the olfactory G-protein -subunit G8. J. Physiol. 591, 3949–3962.

Murray, R.C., Navi, D., Fesenko, J., Lander, A.D., Calof, A.L., 2003. Widespread defects in the primary olfactory pathway caused by loss of Mash1 function. J. Neurosci. 23, 1769–1780.

Nakano, H., Iida, Y., Suzuki, M., Aoki, M., Umemura, M., Takahashi, S., Takahashi, Y., 2016. Activating transcription factor 5 (ATF5) is essential for the maturation and survival of mouse basal vomeronasal sensory neurons. Cell Tissue Res. 363, 621–633.

Oboti, L., Ibarra-Soria, X., Perez-Gomez, A., Schmid, A., Pyrski, M., Paschek, N., Kircher, S., Logan, D.W., Leinders-Zufall, T., Zufall, F., Chamero, P., 2015. Pregnancy and estrogen enhance neural progenitor-cell proliferation in the vomeronasal sensory epithelium. BMC Biol. 13, 104.

Patel, T., Hobert, O., 2017. Coordinated control of terminal differentiation and restriction of cellular plasticity. Elife 6.

Pinto, L., Drechsel, D., Schmid, M.T., Ninkovic, J., Irmler, M., Brill, M.S., Restani, L., Gianfranceschi, L., Cerri, C., Weber, S.N., Tarabykin, V., Baer, K., Guillemot, F., Beckers, J., Zecevic, N., Dehay, C., Caleo, M., Schorle, H., Gotz, M., 2009. AP2gamma regulates basal progenitor fate in a region- and layer-specific manner in the developing cortex. Nat. Neurosci. 12, 1229–1237.

Prince, J.E., Cho, J.H., Dumontier, E., Andrews, W., Cutforth, T., Tessier-Lavigne, M., Parnavelas, J., Cloutier, J.F., 2009. Robo-2 controls the segregation of a portion of basal vomeronasal sensory neuron axons to the posterior region of the accessory olfactory bulb. J. Neurosci. 29, 14211–14222.

Silvotti, L., Moiani, A., Gatti, R., Tirindelli, R., 2007. Combinatorial co-expression of pheromone receptors, V2Rs. J. Neurochem. 103, 1753–1763.

Srinivas, S., Watanabe, T., Lin, C.S., William, C.M., Tanabe, Y., Jessell, T.M., Costantini, F., 2001. Cre reporter strains produced by targeted insertion of EYFP and ECFP into the ROSA26 locus. BMC Dev. Biol. 1, 4.

Stein, B., Alonso, M.T., Zufall, F., Leinders-Zufall, T., Chamero, P., 2016. Functional overexpression of vomeronasal receptors using a herpes simplex virus type 1 (HSV-1)-derived amplicon. PLoS One 11, e0156092.

Suarez, R., 2011. Molecular switches in the development and fate specification of vomeronasal neurons. J. Neurosci. 31, 17761–17763.

Tirindelli, R., Ryba, N.J., 1996. The G-protein gamma-subunit G gamma 8 is expressed in the developing axons of olfactory and vomeronasal neurons. Eur. J. Neurosci. 8, 2388–2398.

Walz, A., Rodriguez, I., Mombaerts, P., 2002. Aberrant sensory innervation of the olfactory bulb in neuropilin-2 mutant mice. J. Neurosci. 22, 4025–4035.

Wakabayashi, Y., Ichikawa, M., 2007. Distribution of Notch1-expressing cells and proliferating cells in mouse vomeronasal organ. Neurosci. Lett. 411, 217–221.

Xu, P.S., Lee, D., Holy, T.E., 2016. Experience-dependent plasticity drives individual differences in pheromone-sensing. Neurons Neuron 91, 878–892.

Yoshihara, S., Omichi, K., Yanazawa, M., Kitamura, K., Yoshihara, Y., 2005. Arx homeobox gene is essential for development of mouse olfactory system. Development 132, 751–762.